Moisture and fungal degradation in fibrous plaster

Zoe C Maundrill[1]
Barrie Dams[1] ORCiD: 0000-0001-7081-5457*
Martin Ansell[1] ORCiD: 0000-0003-2946-1735
Daniel Henk[2] ORCiD: 0000-0002-1142-3143
Emeka K. Ezugwu[1]
Marion Harney[1] ORCiD: 0000-0003-1931-3149
John Stewart[3] ORCiD: 0000-0001-6292-3191
Richard J Ball[1] ORCiD: 0000-0002-7413-3944

[1]*Department of Architecture & Civil Engineering, University of Bath, Claverton Down, Bath, BA2 7AY, United Kingdom.*
[2]*Department Biology and Biochemistry, University of Bath, Claverton Down, Bath, BA2 7AY, United Kingdom.*
[3]*Historic England, 4th Floor, Cannon Bridge House, 25 Dowgate Hill, London EC1R 2YA United Kingdom.*

*Corresponding author: Barrie Dams bd272@bath.ac.uk

Abstract

Fibrous plaster degradation has been a key concern over recent years, with ceiling failures occurring suddenly in historic buildings, including the Apollo theatre in 2013. This rigorous investigation explores fibrous plaster degradation through subjecting 290 specimens to a range of moisture and fungal-related treatment conditions over periods of up to two years and analysis using mechanical flexural tests, Fourier Transform Infrared Spectroscopy (FTIR), Scanning Electron Microscopy (SEM) and Deoxyribonucleic Acid (DNA) sequencing. Using FTIR peak ratios from spectra of hessian fibres and mechanical tests in conjunction, an original methodology for identifying mechanisms and severity of fibrous plaster degradation through moisture and fungal exposure was developed. Results showed defined clusters for differing moisture and fungal treatments when two peak ratios are plotted together and compared with mechanical data. Fungal exposure over two years, water submersion and wetting and drying were particularly detrimental conditions for fibrous plaster. Fungal exposure resulted in degradation of cellulose bonds in hessian fibres, with defined clusters on the extreme left of peak ratio plots correlating with a pronounced reduction in fibrous plaster mean flexural strength of 51%. Fungal species *Penicillium* and *Chaetomium* were identified on test samples. Moisture affected plaster matrices significantly with wetting/drying and water submersion treatments resulting in a 71% reduction in mean flexural strength for unreinforced plaster, reducing to 26% with hessian-reinforced fibrous plaster. Many buildings containing fibrous plaster are listed and removal of material is often minimised - the high impact of this research stems from the ability to rapidly assess the mechanical integrity of a very small quantity of harvested historic hessian fibres using FTIR. Identifying the location of weakened fibres in a ceiling is highly important for effective restoration and conservation.

Keywords— Fibrous plaster, Hessian Fibres, Degradation, Fungi, Moisture, Fourier Transform Infrared Spectroscopy (FTIR), Scanning Electron Microscope (SEM), Deoxyribonucleic Acid (DNA).

Glossary

ANOVA	Analysis of Variance
BLAST	Basic Local Alignment Search Tool
DNA	Deoxyribonucleic Acid
FASTA	Used in DNA testing, a text based format representing sequences
FE	Fracture Energy
FTIR	Fourier Transform Infrared Spectroscopy
ITS	Internal Transcribed Spacer
LOP	Limit Of Plasticity
MOE	Modulus of Elasticity
MS	Maximum Stress
PDA	Potato Dextrose Agar
SEM	Scanning Electron Microscopy

1 Introduction

Fibrous plaster has been used as a material in buildings for well over a century and is perhaps best known for providing decorative interiors and ornate ceilings in buildings such as theatres, hotels, civic buildings and private residences [1]. In a theatre setting, fibrous plaster ceilings typically are found above the auditorium and form part of a large and complex building structure as shown in Figure 1. Human occupation and activity can vary considerably within venues and contribute to the fibrous plaster ceiling experiencing differences in temperature, relative humidity, sound vibration and presence of micro-organisms in the air both below the fibrous plaster ceiling and above in the roof-space, where fibrous plaster ceilings are also subject to external weather conditions through the envelope of the roof structure.

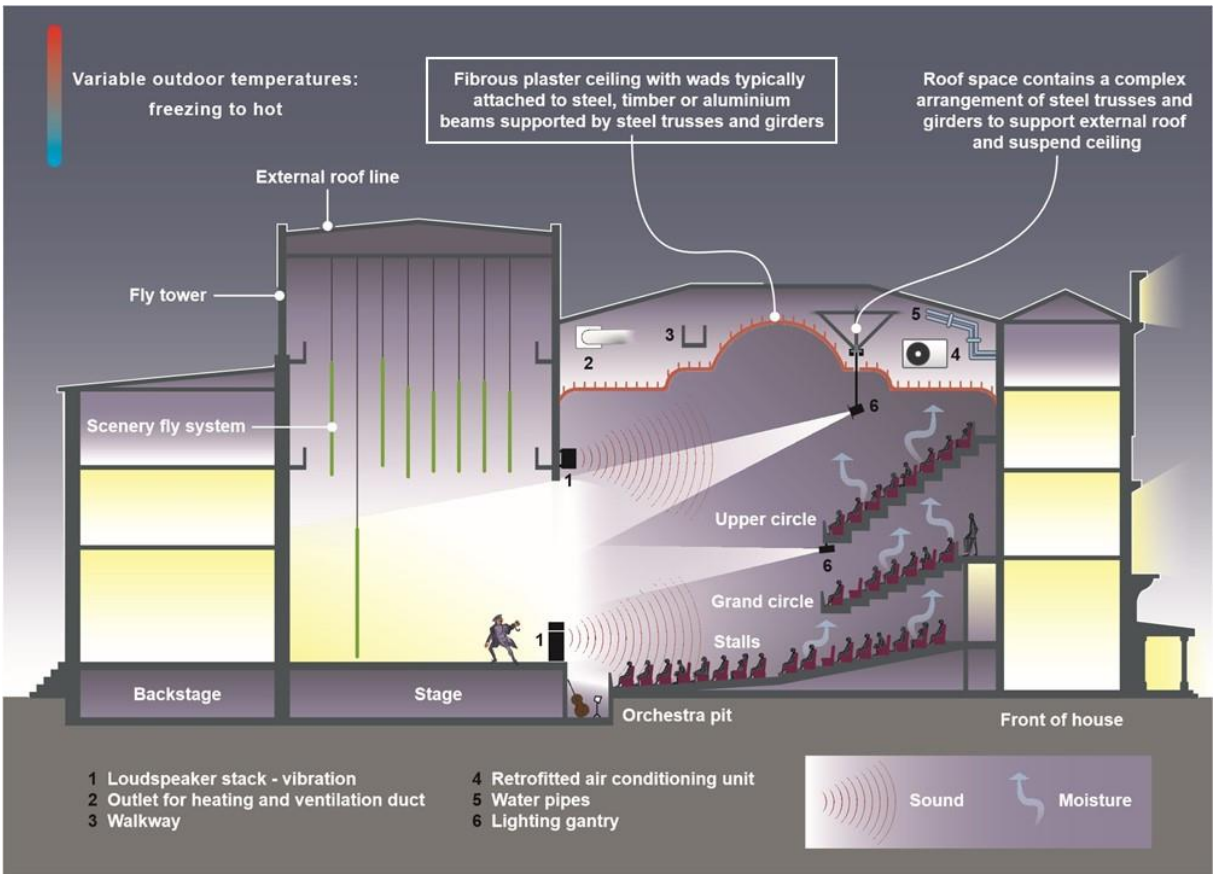

Figure 1 - Cross sectional diagram of a typical theatre layout, with the fibrous plaster ceiling hung above the auditorium and subjected to varying environmental conditions resulting from human occupancy and external weather (Image courtesy of Historic England)

Failures have occurred in historic fibrous plaster applications during the 21st century which has drawn more attention to fibrous plaster ceilings in particular, with the most notable and widely publicised failure occurring during a performance at the Apollo theatre, London, in 2013 [2] where 58 people were hospitalised through injury attained through fallen fibrous plaster debris from a partial ceiling collapse [3]. The Savoy Hotel, London, also had a similar, but smaller-scale, event in 2019 when a collapse happened during a charity auction event [4] and the Piccadilly theatre also experienced a partial collapse in 2019 [5].

Failure incidents such as the above accentuate the importance of identifying and understanding the mechanisms of degradation in fibrous plaster ceilings with a view to assisting and informing the practice carrying out appropriate maintenance and repair work on

an ongoing basis; in the wake of the Apollo Theatre collapse, it is required for places of entertainment to be inspected by industry specialist plaster companies and structural engineers for deterioration on a regular basis [6]. Is it important to conduct research into identifying the extent to which potential failure mechanisms resulting from differing environmental conditions can affect and influence the degradation of fibrous plaster over time.

Decorative plaster was originally made from a combination of lime mortar and animal hair. Gypsum plaster (also known as 'Plaster of Paris') subsequently became a popular alternative to lime, which was ultimately quicker to set, lighter, and facilitated an increase in production speed [2]. Hessian fibre scrim, typically comprising of bundled bast fibres from the jute plant [1] became the most common reinforcement material within the gypsum plaster matrix. Leonard Alexander Desachy patented the gypsum plaster and hessian fibre combination as fibrous plaster in 1856 [7]. Gypsum plaster consists of three phases - calcium sulfate dihydrate ($CaSO_4.2H_2O$), calcium sulfate hemihydrate ($CaSO_4.0.5H_2O$), and calcium sulfate anhydrite ($CaSO_4$), with the proportions of each determining the gypsum plaster properties [8]. Traditional gypsum plaster (known as 'beta' plaster) possesses an uneven crystalline structure [9], [8]. Gypsum plaster is a brittle material but the addition of fibrous reinforcement improves ductility and durability [10].

To date, there has not been a large quantity of research conducted explicitly on fibrous plaster and only a select group of specialist practitioners across the United Kingdom possess the expertise to maintain fibrous plaster ceilings. Guidance written by Stewart et al., 2019 provides a history of fibrous plaster, details forms of degradation and gives advice concerning methods of care and repair [1]. Ireland, 2020 published guidance on the assessment and repair of fibrous plaster ceilings [11]. Ngah et al., 2020 conducted research on the strength of gypsum plaster, hessian fibres and quadaxial and continuous fibre mat glass fibre reinforcement as potential modern substitutes for hessian fibres [8]. The Institute of Structural Engineers published two articles providing a comprehensive overview of the potential causes of failure of historic fibrous plaster ceilings, including a methodology for carrying out *in-situ* assessments of condition [5], [12].

Moisture (including water ingress and variable humidity) and fungal growth have been identified as important fibrous plaster degradation mechanisms, whether via biodegradation of the hessian fibre scrim or compromising the integrity of the gypsum plaster matrix. Hessian scrim is a natural fibrous material which does not bind strongly with gypsum plaster [8]; this may promote degradation (and ultimately failure) by allowing fungal growth and/or moisture ingress within cracks and voids. Moisture and fungi may even be introduced to hessian fibres at the early stage of retting (fibre separation from plant stem) which uses several different methods (plus possible treatment with caustic soda) involving moisture and microbes [13], [14].

Moisture may degrade gypsum by two possible methods; either gypsum will dissolve over time, weakening the material and ultimately leading to failure, or moisture acts as a lubricant by allowing gypsum particles to slide over each other. Gypsum crystals are randomly orientated and are a mosaic of different textures [15] and dimensionally varied, therefore the dissolution surface is uneven and unpredictable [16]. Gypsum dissolution by moisture over time could be a factor which influences the rate of degradation [16] allowing not only moisture to affect gypsum strength but also provide a shorter route for moisture reaching internal fibres (though the research was not explicitly concerning fibrous plaster). With fibres situated inside a porous gypsum matrix, moisture is transferred more easily to fibres through the interface [17]. Moisture degrading flax fibres inside a resin epoxy matrix was noted by Assarar et al., 2011 who concluded that matrix-interface weakening was the main cause of failure [17].

Moisture is known to affect natural bast fibres due to the high absorption ability of cellulose [13]; hydroxyl groups within fibres attracting water molecules through the formation of

hydrogen bonds. Cellulose and lignin ratios of the reinforcement fibre determine the level of water absorption; jute has a relatively high lignin content (11% - 26%) and lower cellulose (45% - 71%) [18] [19] which promotes higher moisture absorption, whereas cotton possesses higher cellulose levels (88% - 96%) [20] and lower lignin content (up to 1%) [21] and absorbs less moisture. Since research explicitly on fibrous plaster is limited, bast fibres are relevant for general comparison as jute and hemp are both types of bast fibres. Research conducted on Flax fibres showed natural fibres are hydrophilic (attracted to water molecules) and composite materials containing them lose strength when subjected to humid conditions [17]. Moisture can infiltrate via several possible mechanisms; diffusion, imperfections or by capillarity in the fibres. Fickian behaviour is likely and moisture equilibrium is reached rapidly in humid conditions and is maintained whilst the humidity remains constant. A flax fibre composite material showed a 13.5% increase in weight when immersed in water whereas there was a 1.05% increase for the glass fibre composite [17]. Bast fibres have high moisture absorption and poor dimensional stability [22] and the swelling of fibres can cause microcracking in surrounding material which in turn leads to degradation. This could be the case for the hessian in fibrous plaster, where swelling due to moisture absorption cracks the plaster, as well as promoting fungal degradation due to the high-humidity environment [22].

Indoor environments need to be carefully controlled and key factors which affect microbial growth are lighting, heating, humidity and ventilation [23] – a challenging task in a venue such as a theatre, which may alternate periods of dense occupation with periods of low or non-occupation. Plaster is known to be affected by fungi within the built environment [23]; it is composed of minerals (gypsum) and is susceptible to biodeterioration. Particulates in the atmosphere are the food source for fungi and bacteria to grow within cracks or pores. Fungi entering the plaster are classed as physical weathering due to filaments growing further into the material. Plaster is classed as a mineral based material so biofilms from the fungi could develop, and humidity could cause mineral dissolution.

Experiments concerning how different environmental conditions affect types of plaster give a good perspective on biodegradation as a result of moisture or fungal-related mechanisms [24]. Fungal growth on gypsum plaster and hessian fibres is facilitated by the porous nature of the materials, with hyphae penetrating the surface of gypsum on a microscopic level [25].

Hessian fibres are organic bast fibres and therefore susceptible to biodegradation by extracellular enzymes [23]. Hessian (jute) fibres were not degraded by fungi when tested as part of a polylactic acid (PLA) composite material, but the PLA was, leading to a gap between the interface and resulting in a loss of strength [26]. Jute fibres by themselves have been heavily degraded by fungi and are susceptible to *Macrophomina phaseolina* pathogens during cultivation [27]. Cladosporium is one of the most densely populated fungi found in both interior and exterior environments [28]. Cellulose is the principal component of bast fibres and provides the basis of strength and stiffness [29]. It has a crystalline structure formed of linear polymer units which in turn form microfibrils held together by hydrogen bonds, forming cellulose fibres which provide tensile strength. However, there is also a varying extent of amorphinity in structure, with enough heterogeneity in topology to allow susceptibility to cellulase - enzymes which can be produced by fungi which decompose cellulose molecules with the mechanism of hydrolysis [30]. Fungi harbour enzymes which break down cellulose into simpler forms (mostly glucose) [31]. Both enzymes and water can be used for the fibre retting process and may affect the natural material. Although retting is a deliberate process that is necessary for fibre extraction, the negative effects of water and fungi in an uncontrolled environment (such as in a ceiling) may be informed by analysing the controlled retting process. It was noted by [22] that moisture combined with fungal growth caused fibres to degrade and lose strength [31]. There are two mechanisms for fungal attack on hessian fibres; either the fungal spores existed on the hessian before it was incorporated into fibrous plaster, or the fungus infiltrated the fibrous plaster during its working life. In the first instance, plaster may appear in good working condition

but fail once the hessian on the inside has degraded. The second mechanism is also possible and may occur alongside the first, causing different species of microbes to enter. One further possibility is purely the plaster cracking and the degradation mechanism being bio-weathering. Fungal spores or moisture already being present in the hessian would cause fibres to degrade.

This study focuses on experimentation and analysis of the degradation of fibrous plaster caused by moisture and fungal growth with the aim of understanding these degradation mechanisms and identifying conditions particularly detrimental to fibrous plaster integrity. Experiments encompassed mechanical flexural testing of plaster specimens with and without hessian fibres, Fourier Transform Infrared Spectroscopy (FTIR) conducted on hessian fibre samples, Scanning Electron Microscopy (SEM) carried out for identification of fungal growth and Deoxyribonucleic Acid (DNA) sequencing of fungal specimens to identify presence upon historic fibrous plaster samples and using this to further inform FTIR analysis of the types of fungi identified.

Improving understanding of degradation mechanisms and anticipating potential failure of fibrous plaster is important for public health and safety, the economic and business operation of the historic buildings in which fibrous plaster is present, and for the wider development of understanding how historic and current construction materials behave when considering in-situ assessment and repair.

2 Methodology

The four-stage investigation strategy of this study consisted of flexural tests of flat plate fibrous plaster specimens, FTIR, DNA and SEM, which together formed a rigorous evaluation of the effects of moisture and fungal growth on the integrity of fibrous plaster. Flexural tests consisted of multiple fibrous plaster plate specimens, subjected to a variety of moisture and fungal-based treatments, tested to failure along with statistical analysis of result variation. Full details of the range of test treatments upon test specimens are presented in section 2.1 and the flexural test method is elaborated upon in section 2.2. FTIR experimentation on hessian fibres subjected to the range of moisture and fungal treatments used a peak ratio method to determine the difference between degradation mechanisms and aid identification of differing moisture and fungal effects; full details of the FTIR method are presented in section 2.5. DNA tests were used to identify types of fungi growing upon exposed samples of hessian fibres, with the methodology outlined in section 2.4 and SEM was used to observe the microstructure of fungal growth upon test specimens as detailed in section 2.3.

2.1 Test sample matrices

Fibrous plaster samples were created and subjected to a variety of environmental treatments, which have been separated into two core categories – moisture treatment and fungal treatment - to assess degradation from both treatments.

2.1.1 Moisture treatments

Table 1 shows the three sub-categories of fibres - no fibrous reinforcement present (N), hessian fibres used (H) and with glass fibres used (G), which were subjected to four moisture-related treatments along with a control category with no moisture treatment process applied. The abbreviations assigned to the combinations of fibre type and moisture treatment are shown and the samples are referred to using these abbreviations hereafter.

Table 1 - Sample matrices for FIBROUS PLASTER samples, both with and without fibres, subjected to moisture-based treatments

Fibrous reinforcement	No treatment (N)	100% RH (H)	Submerged in water (W)	Wetting and drying (D)	Freeze thaw (T)
None (N)	NN	NH	NW	ND	NT
Two Layers of Hessian (H) fibres (1 mm from sample base)	HN	HH	HW	HD	HT
Two Layers of Glass (G) fibres (1 mm from sample base)	GN	GH	GW	GD	GT

For the 100% humidity tests, the sample specimens were stored for three months in a closed plastic container. 4000 ml of water was inside the container, creating the humid environment with a stainless-steel mesh holding the samples at a level of 100 mm above the surface of the

water. Submerged in water tests involved the samples being submerged in a closed container with water for seven days [32]. Both methods are illustrated in Figure 2.

During the wetting and drying tests, samples were placed in a chamber which contained shelving, an extractor fan, timer, and water nozzle. The samples were sprayed continuously for 18 minutes, followed by a fan-drying phase lasting the remaining 23 hours and 42 minutes of each day (Figure 2). This process was repeated 30 times overall [32].

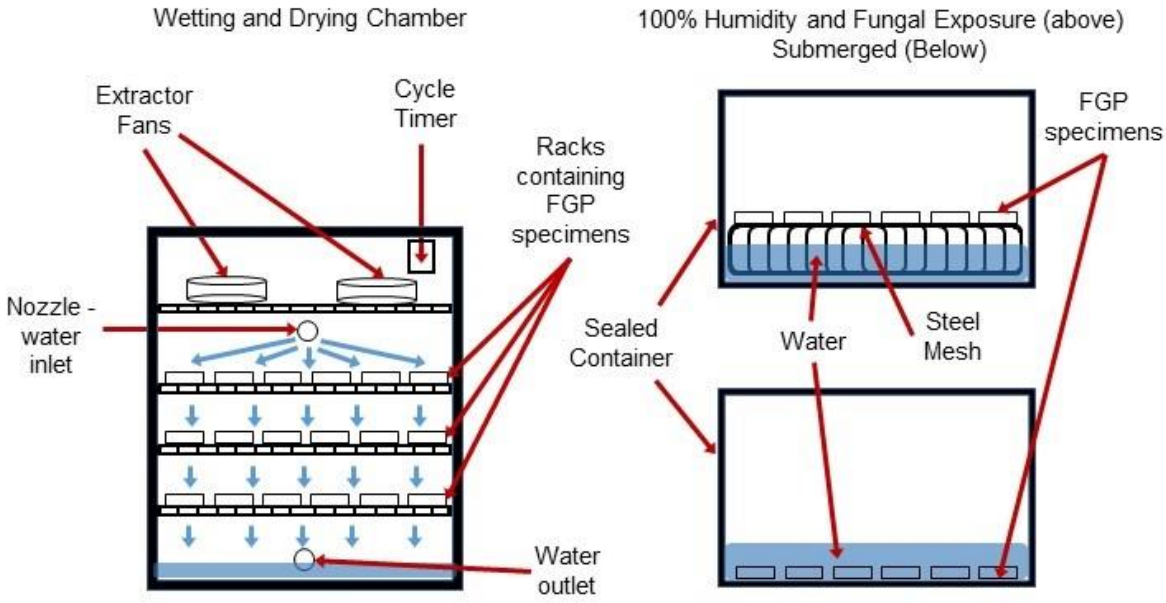

Figure 2 - Diagrams illustrating the methodologies for the wetting and drying treatment (left) and the 100% Relative Humidity, Fungal exposure and submerged methods (right)

Samples subjected to the freeze-thaw conditions were first placed in tap water until a constant weight was reached, indicating the pores were full of water, then the excess water was wiped from the outside with a dry cloth. Following this, they were transferred to a freezer for 36 hours before being dried on cotton fabric covers on top of a heated surface at 50°C until the weight remained constant. This final sample weight was lower than the original weight due to some of the gypsum dissolving during the process and this freeze thaw condition cycle was completed once for each sample [32].

2.1.2 **Fungal treatments**

Table 2 shows the three sub-categories of specimens, both with hessian fibres (in two different configurations) and without, which were subjected to three fungal-related treatments and a control category with no treatment. The table shows the allocated sample abbreviations which are used in the results sections.

For the treatment category of subjecting new fibrous plaster samples to fungi without a food source, historic fibrous plaster samples obtained from the Hammersmith Apollo and KOKO Theatre, (supplied by specialist plaster companies Hayles and Howe, Bristol, and Locker and Riley, South Woodham Ferrers) were used for creating conditions in which fungal spores were present. These historic samples were placed on a stainless-steel mesh with the new flexural samples manufactured for testing within a sealed container as used for the 100% humidity

tests, with 4000 ml water at the bottom of the container (Figure 2). The samples were then kept in these conditions for three months [32].

Table 2 - Sample matrices for FIBROUS PLASTER samples, both with and without fibres, subjected to fungal-based treatments

Fibrous reinforcement	No treatment	Exposed to Fungal spores		
		3 months		24 months
	No food source	No food source	food Source	food source
	(N)	**(F)**	**(Ff)**	**(F2)**
None **(N)**	NN	NF	NFf	NF2
Two Layers of Hessian fibres 1mm Away from sample base **(A)**	AN	AF	AFf	AF2
Two Layers of Hessian fibres next to sample Base **(B)**	BN	BF	BFf	BF2

Condition exposure for the samples exposed to fungus with a food source involved a similar method to those exposed without a food source, but with the addition of malt extract with 1 gram added per 100 ml water in the sealed container for three months [32]. The two-year samples (NF2, AF2 and BF2) were then kept under these conditions within a sealed container for a period of two years.

2.2 Three point flexural tests

Fibrous plaster specimens for three-point flexural tests were manufactured using Siniat Prestia Classic Beta plaster. Hessian (jute fibre) scrim reinforcement with a variable mesh size of 5 mm x 5-10 mm (typically 7 mm) and a weight of 102 g/m^2 [33] was set inside the gypsum plaster matrix in two layers (distance from base surface as detailed in Table 1 and Table 2). For comparison, specimens were also made using continuous glass fibre mats with a weight of 210 g/m^2. The plaster matrix was cast in moulds with dimensions of 100 mm x 40 mm x 5 mm. Flexural strength tests on the samples involved a three-point bend test with a 50 kN load cell in an Instron 3366 Universal testing machine applying a central point load at a displacement rate of 0.5 mm/min (as shown in Figure 3, along with images of failure both with and without fibrous reinforcement). Displacements were recorded every 0.1 seconds until a 1.5 mm displacement was reached, with the rate then increasing to 5 mm/min until a total displacement of 10 mm had been applied. Under each condition shown in the sample test matrices in Table 1 and Table 2, there were twelve flexural samples manufactured and tested to identify variation in the results by statistical analysis.

Four parameters were determined for comparison and evaluation – the maximum stress (MS), flexural Modulus of Elasticity (MOE), Limit of Plasticity (LOP) and Fracture Energy (FE). The parameters were calculated from each of the twelve samples from each combination shown in Table 1 and Table 2, following which a mean value was taken for that data set of twelve samples.

From the load (kN) and displacement (mm) data, stress and strain were calculated. Maximum stress σ was obtained using equation (1) from International standards concerning flexural strength [34]:

$$\sigma = \frac{3PL}{2bd^2} \quad (1)$$

where P is the maximum load (kN), L is the length of the span from centre to centre of the support rollers (mm), b is the breadth of the test sample (mm) measured using digital callipers and d is the depth of the test sample (mm) measured using digital callipers. Flexural strain ε was calculated using equation (2):

$$\varepsilon = \frac{6Dd}{L^2} \quad (2)$$

where D is the deflection of the sample (mm), d is the depth of the sample (mm) and L is the length from centre to centre of the support rollers (mm). Limit of Plasticity (LOP) is taken as the point at which a material ceases to behave in the linear elastic range. Typically, in samples which have no fibrous reinforcement, this is the same as the maximum stress. Flexural Modulus of Elasticity MOE was calculated using equation (3):

$$MOE = \frac{SL^3}{4000bd^3} \quad (3)$$

where S is the slope (or gradient) of the initial linear portion of the initial force (N) verses displacement (mm) curve and L, b and d are length, breadth, and depth as for equation (1) (mm). Fracture Energy FE (kJm^2) can be defined as the energy required to change a unit area of a fracture surface from its initial unloaded state to a state of complete separation and was calculated using equation (4) based upon the work of Petersson [35], [36] and Khalilpour et al. [37]:

$$FE = \frac{E + Mg\delta_0}{b(d - a)} \quad (4)$$

where E is the Fracture Energy (Nmm) calculated as the area under the stable load (N) versus deflection (mm) curve (not stress verses strain) until the point of deflection at maximum load; this was calculated using the trapezium method and approximated the areas between two sets of data points and summing to obtain the total area, b and d (mm) are breadth and depth respectively; a represents the notch cut (mm) if one was present (as there was no notch cut into these small fibrous plaster test samples, the value of a was zero) and $Mg\delta_0$ is a correction factor to allow for the mass of the beam; this would be required when dealing with a beam of notable mass such as concrete due to the length of the beam protruding over the end support of the rollers, being less than ¼ of the length of the beam [37]. M is the mass of the beam (kg), g is gravity taken as 9.81 ms^{-2} and δ_0 is the deflection of the test sample at maximum applied load (mm). However, in this study the mass of the fibrous plaster flexural samples led to this correction factor to be considered negligible, and therefore not applied.

To provide statistical analysis of the flexural test results for samples subjected to moisture and fungal treatments, two statistical methods were chosen: Analysis of Variance (ANOVA) single factor and student t-test distributions (two-sample assuming unequal variances). These tests take the mean and variance into account, giving a more reliable result than using one statistical value. The null hypothesis was *'enough evidence to suggest the values are similar'*. A value of 0.05 was used for the significance level alpha α for both statistical tests, meaning the null hypothesis was accepted if the comparison value exceeded 0.05.

The ANOVA method has previously been used for analysing flax fibres and assessing how variations in chemical treatments impacted upon mechanical properties [38]. In this study, entire sample sets were initially tested using the ANOVA method, with sample size reducing

(down to a minimum of three) to determine how many samples within a particular treatment set led to the null hypothesis being accepted. The t-test method was then applied to compare the similarity between two samples within a treatment category and assess whether the null hypothesis was accepted for the two samples.

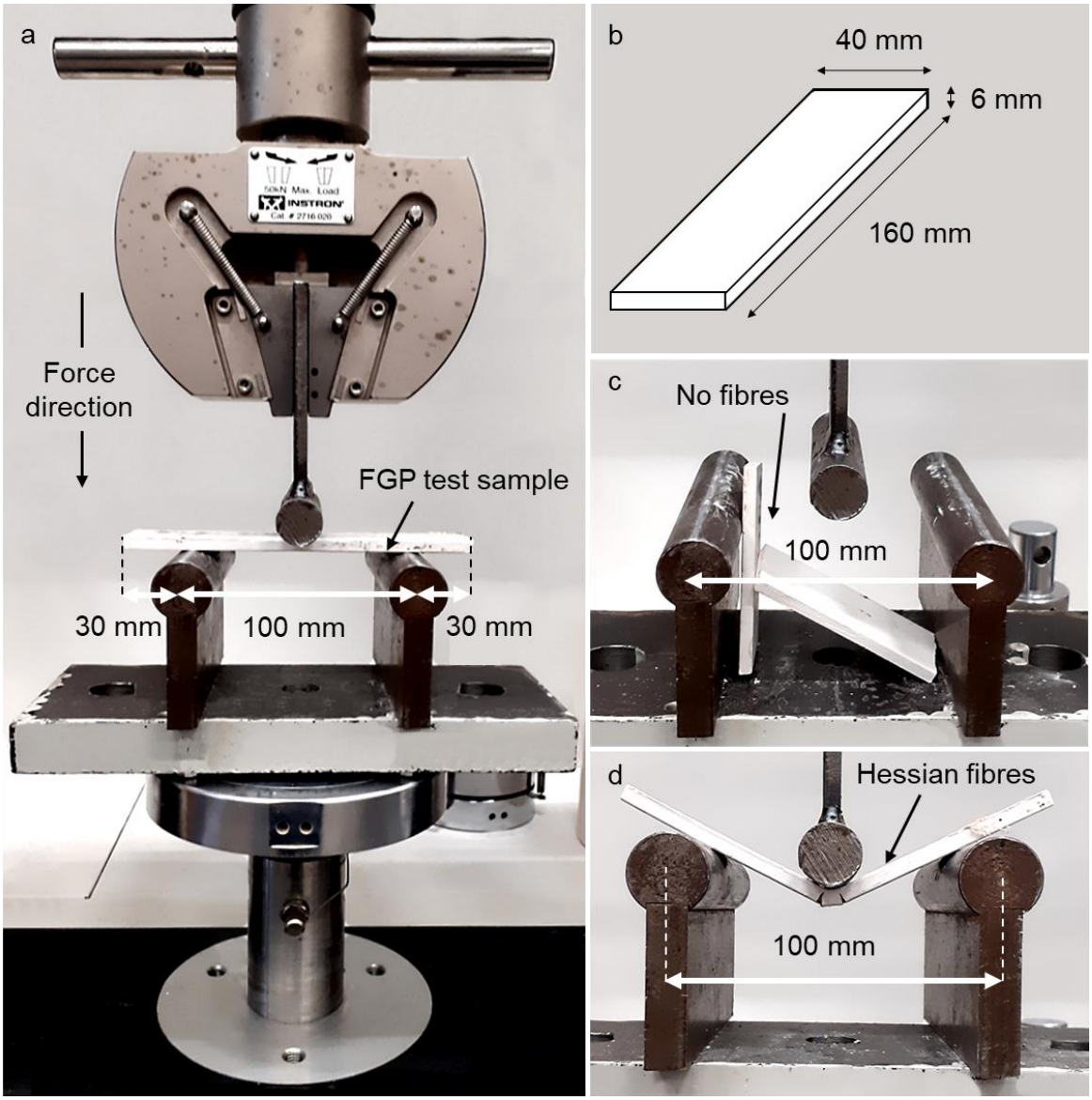

Figure 3 – Flexural test specimens and test set-up, a) a specimen loaded in the three-point test rig, b) Dimensions of the flexural test specimens, c) A typical failure of a specimen without fibrous reinforcement and d) a typical sample with hessian fibre reinforcement.

2.3 Scanning Electron Microscopy (SEM)

To obtain microscopic observation of the growth of the fungus on sample specimens, SEM imaging was undertaken on samples subjected to three different conditions:

- 100% relative humidity (HH)
- samples with historic hessian exposed to fungi with a food source (BFf)
- samples with historic hessian exposed to fungi without a food source (BF)

All samples were placed on a 50 mm diameter aluminium mount and kept under vacuum for 48 hours prior to being covered in a 10 nm gold sputter coating in order to reduce charging before insertion into the microscope chamber. The SEM imaging was carried out to identify the fungus type and the pattern of growth on the gypsum plaster and hessian fibre scrim material. Images were captured with a JEOL SEM6480LV microscope at various magnifications.

2.4 DNA fungal identification

Historic fibrous plaster samples, with the historic hessian fibres exposed were used for the identification of fungus growing within the reinforced fibrous plaster samples. The preparation process involved the sample specimens being submerged for ten seconds in a 2.5% hypochlorite solution, followed by placing for ten seconds in a 70% ethanol rinse and finally being washed for forty seconds in distilled water.

Following this procedure, sample specimens were divided using forceps, whilst ensuring each piece had internal hessian fibres exposed on at least one side and were each placed on a section of a Potato Dextrose Agar (PDA) to promote fungal growth. Incubation time for the samples was at least 3 days at a temperature of 25°C. Fungi which grew under the conditions were then transferred to separate plates for analysis. Any fungi growing on test plates in areas surrounding fibrous plaster sample specimens was not tested.

The most widely used DNA barcode region for fungus identification was amplified using Internal Transcribed Spacer (ITS) 1 and ITS4 primers and this was sequenced using ITS1 for undertaking Eurofins mix2seq sequencing. FASTA (a text-based format) sequences were then trimmed and used with the Interactive Basic Local Alignment Search Tool (BLAST) on the fungal ITS database for identification of the fungal species. The BLAST results were stored as a text file which was then manually compared to the results on the database. Identification of fungal species was based on the similarity to, or match with, DNA sequences already contained in a sample database.

The most common fungi identified from the DNA tests were then grown in a petri-dish, with the food source, and FTIR samples obtained for both mould and food source, the spectra of which were compared to the hessian samples and similarity, or dissimilarity of spectra peaks observed.

2.5 Fourier Transform Infrared Spectroscopy (FTIR)

Hessian fibres were extracted from a flexural test specimen for every different exposure condition as described in Table 1 and Table 2. A Perkin Elmer Frontier FTIR instrument with a diamond Attenuated Total Reflectance head was used for the scans. A Mercury-Cadmium-Telluride (MCT) detector cooled by liquid nitrogen was used for the mid-infrared sensitivity and provides a better response for the low levels of energy reaching the detector. The scan resolution was 4 cm^{-1} with a wave number range from 600 cm^{-1} to 4000 cm^{-1}. 32 scans were completed for each sample to obtain a high resolution, enabling significant peaks to be identified. Extracted fibres were placed in a horizontal alignment on the crystal. Before each scan of a different condition, a background scan was completed and the instrument was cleaned with distilled water between every scan.

Based upon the FTIR peak ratio work of Garside and Wyeth [18] , a method using FTIR peak ratios (R) (attained by the division of a transmittance peak value at a certain wavelength by the peak at another wavelength) was adapted for this study, with two peak ratios named R_1 and R_2 plotted on an *x* and *y* axis to determine the identification of cellulosic fibres. It was aimed that multiple R_1 and R_2 results from different samples plotted on the same graph would indicate clusters or trends within the moisture and fungal treatment category sample sets with a view to differentiating the mechanisms of degradation. Peak ratios at the wavelengths shown in equations (5) and (6) were selected and used by this study:

$$R_1 = \frac{I_{1735}}{I_{1105}} \tag{5}$$

$$R_2 = \frac{I_{1735}}{I_{2900}} \tag{6}$$

Where I_{1105} is the wavelength peak (dotted line in Figure 2) at 1105 cm^{-1} indicating the C-O-C glycosidic bond representing cellulose content and I_{2900} is the wavelength peak height at 2900 cm^{-1} denoting the C-H bond representing a measure of overall organic content [18]. The main constituents of fibrous plants are cellulose, hemi-cellulose, lignin and pectin. Pectin content determines the flexibility of fibrous plants; pectin is water soluble and degradable, which can cause fibres to lose overall strength [29]. The peak at wavelength 1735 cm^{-1} representing pectin (C=O ester bond), was used in this study as the numerator I_{1735} in equations (5) and (6) rather than the peak at 1595 cm^{-1} (C=C aromatic in-plane, representing lignin content) used in Garside and Wyeth, 2003 (which resulted in relative insensitivity as to whether samples were modern or aged). A wavelength of 1735 cm^{-1} showing pectin is reported as being clearer in degraded materials from the carboxyl groups in oxycelluloses [18]. Therefore, in this study R_1 and R_2 represent pectin to cellulose and pectin to overall organic material ratios respectively.

For each chosen wavelength peak, a baseline was estimated, and the peak intensity was calculated using the transmittance at the peak top, as well as the transmittance at the wavelength along a linear baseline using $y = mx + c$. Figure 4 shows an example of an FTIR plot with peak transmittance for a sample set in the HN (top) treatment category showing the application of the linear baseline for the three peak wavelengths, calculated and applied to the peak ratios in equations (5) and (6).

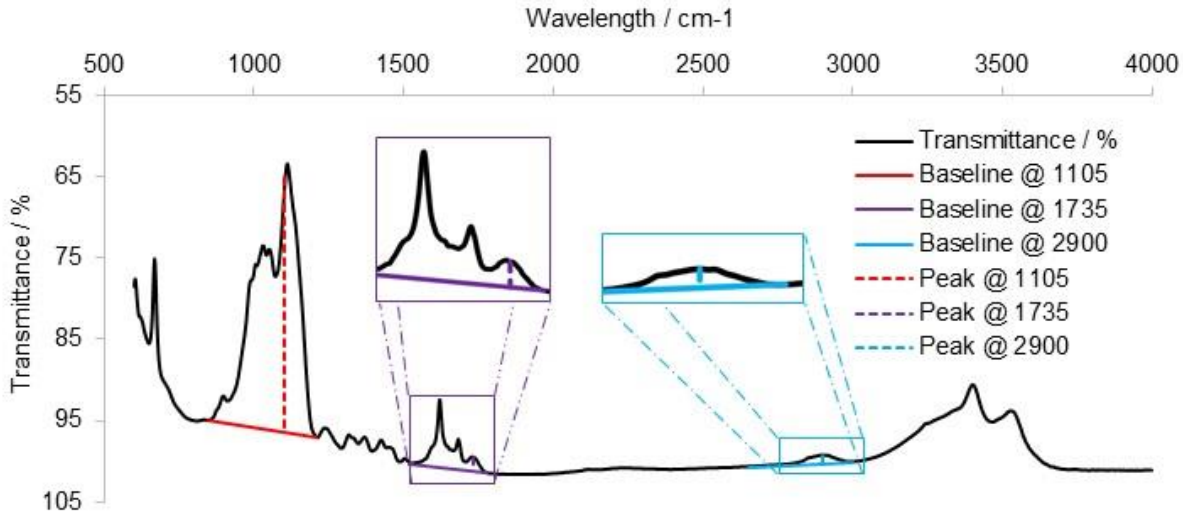

Figure 4 – Example FTIR plot showing peak transmittance and linear baselines applied for a fibre in treatment category HN.

3 Results

3.1 Three point flexural tests

The three point flexural tests for both the moisture treated and fungal growth-treated samples are shown in Figure 5 Part 1 (specimens with no fibres and glass fibres) and Part 2 (specimens with hessian fibres) - note the differing vertical axis for glass fibre specimens and the different horizontal axis for specimens with no fibres. Maximum Stress (MS, MPa), Limit of Plasticity (LOP, MPa), Modulus of Elasticity (MOE, GPa) and Fracture Energy (FE, KJ/m^2) are shown for each moisture and fungal treatment category. Figure 6 shows a selection of the flexural specimens subjected to the two-year fungal treatments after testing and reveals the extent to which fungal growth can be observed on the exterior of the fibrous plaster matrix Particularly AF2 specimens in part (*c*), and the variability from specimen to specimen, with black growth being a clear visible sign of fungal attack [23].

Of particular note is the growth observed on AF2 specimens; sample specimens subjected to fungi from historic samples (NF, AF and BF series) and samples subjected to 100% RH (NH, HH, GH) also displayed fungal growth. Table 3 shows the t-test results for the flexural samples and how two samples relate to one another within the treatment category, with green indicating the acceptance of the null hypothesis and grey rejection of the null hypothesis. Running ANOVA tests for each moisture and fungal treatment category in Table 1 and Table 2 results in the null hypothesis largely being rejected for the full range of samples within the treatment category. The most notable differences are noted in the mechanical property subsections below.

3.1.1 Maximum Stress (MS)

For maximum stress (MS), the tests on fibrous samples were continued until a displacement of 10 mm was reached. For the samples which do not possess fibrous reinforcement (NN, NH, NW, ND, NT, NF, NFf, NF2) the limit of plasticity (LOP) equals MS. Unreinforced samples were affected by the conditions in mechanical testing results. Samples which were submerged in water (NW, 71.2% decrease compared to the no treatment samples with ANOVA analysis), subjected to wetting and drying tests (ND, 43.3% decrease compared to no treatment) and subjected to fungus for two years (NF2, 42.6% compared to no treatment) impacted the plaster the most.

Hessian-reinforced plaster tests resulted in the samples exposed to historic fibres with fungi and no food (BF) having a higher maximum stress than the no-treatment samples (NF) when the reinforcement was located almost at the bottom of the sample. Otherwise, ANOVA analysis reveals AF2 samples (51.4%), HW (25%) and HD (35%) were the most negatively impacted with a decrease for each average maximum stress value compared to the no-treatment samples.

The glass fibre samples (GN, GH, GW, GD, GT) were also all affected by the environmental conditions, to the point of rejecting the null hypothesis, with submerged in water (GW) and wetting and drying (GD) being the most affected with a 56.7% and 44.2% decrease in maximum stress respectively compared to no treatment.

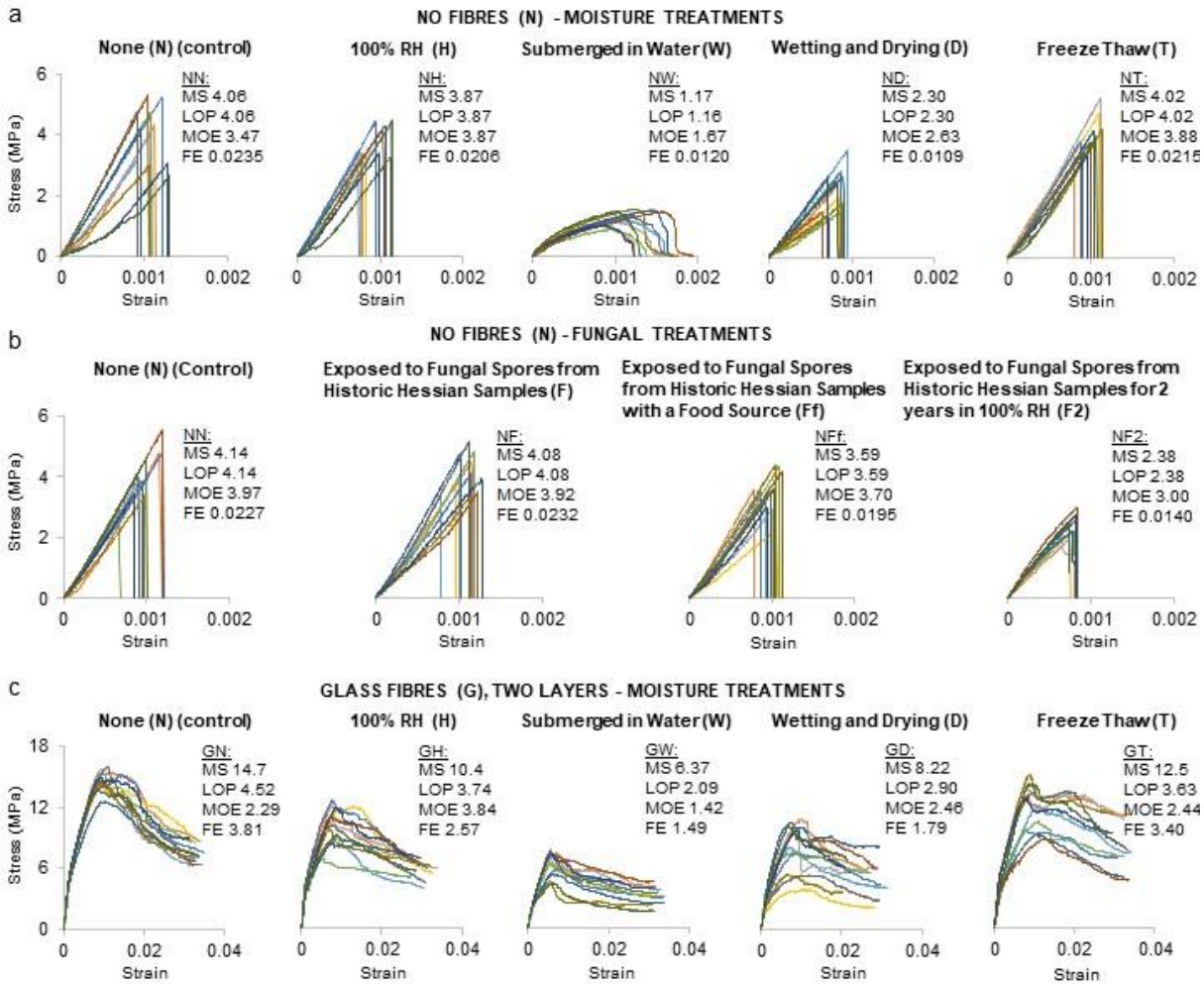

Figure 5 Part 1 - Three point flexural test results – No Fibres and Glass Fibres, which shows a) the moisture treatment results for specimens with no fibres, b) fungal treatment results for specimens with no fibres and c) moisture treatment results for specimens with glass fibres. All three sample groups show results for Maximum stress (MS, MPa), Limit of Plasticity (LOP, MPa), Modulus of Elasticity (MOE, GPa) and Fracture Energy (FE, KJ/m^2). Glass fibre specimens were not subject to fungal treatment.

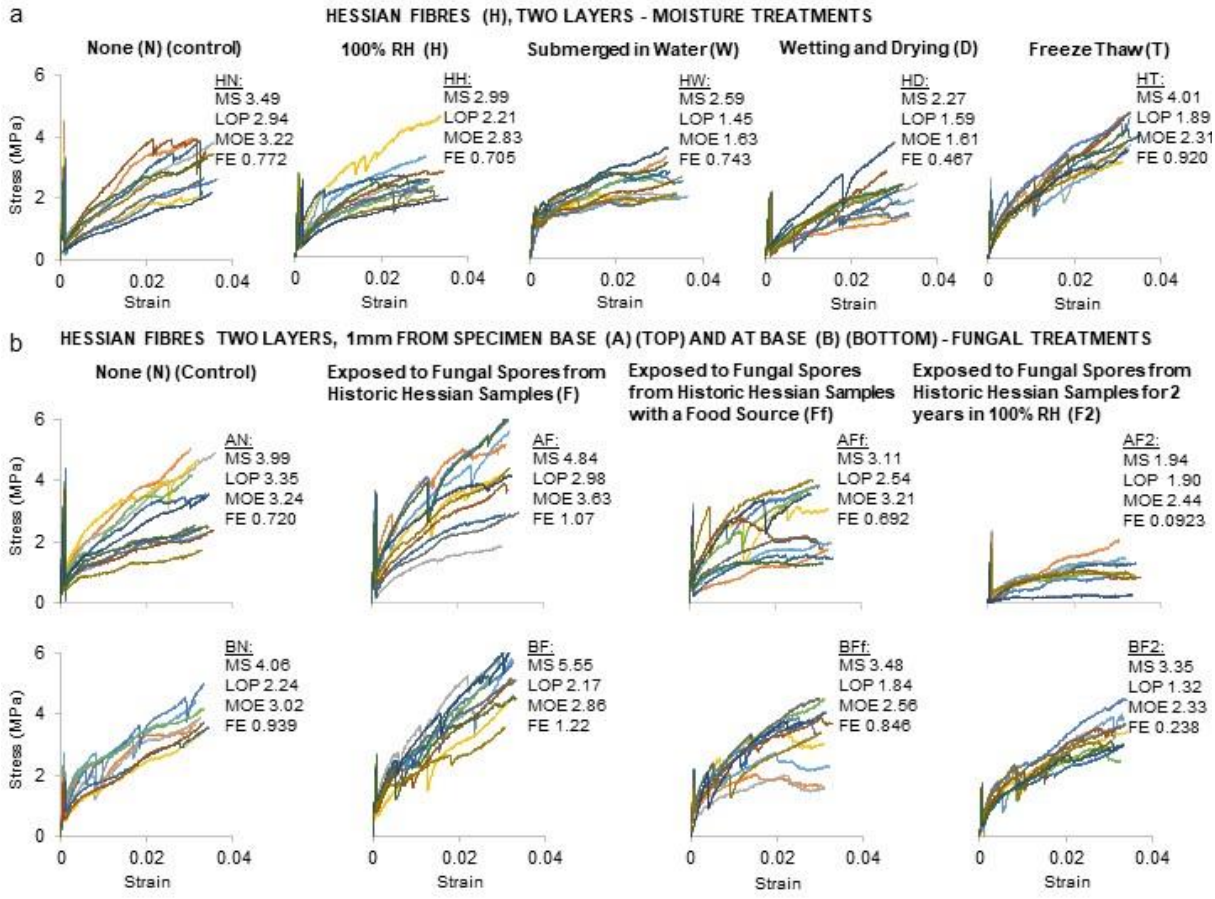

Figure 5 Part 2 - Three point flexural test results – Hessian Fibres, which shows a) the moisture treatment results for specimens with two layers of hessian fibres, b) fungal treatment results for specimens with two layers of hessian fibres 1mm from the bottom of the specimen bases (top) and two layers of hessian fibres right at the specimen bases (bottom). All three sample groups show results for Maximum stress (MS, MPa), Limit of Plasticity (LOP, MPa), Modulus of Elasticity (MOE, GPa) and Fracture Energy (FE, KJ/m2).

Figure 6 - Flexural test specimens subjected to the two-year fungal treatment showing the extent to which fungal growth can be observed on the exterior of the fibrous plaster, and the variation in extent within samples. a) NF2 – no treatment, no fungal growth evident. b) BF2 – subjected to fungal treatment, some growth evident. c) AF2 – subjected to fungal treatment and shows very significant fungal presence on the sample specimens.

3.1.2 **Limit of Plasticity (LOP)**

For the unreinforced samples, the results are the same as the maximum stress due to the brittle failure of the gypsum and ensuing stress-strain profile. All conditions affected the limit of plasticity in the samples with hessian reinforcement so the null hypothesis could not be accepted for any conditions, with submerged in water being the most greatly affected (HW, 50.7% decrease from HN), wetting and drying (HD), freeze-thaw (HT) and then 100% humidity (HH) the least affected (24.8% decrease) in comparison to HN. The addition of the food source to historic fungi and keeping samples exposed to fungi for two years clearly impacted the performance of the samples with hessian in mechanical testing, with samples subjected to fungi for two years showing a reduce LOP (43% for AF2 and 41% for BF2) in comparison to NF2. Again, for the glass fibre reinforced samples, the LOP was negatively affected compared to the control for every environmental condition, with a 53.8% mean decrease for submerged in water and 35.8% decrease for wetting and drying.

3.1.3 **Modulus of Elasticity (MOE)**

The modulus of elasticity for the no-reinforcement samples subjected to moisture treatments was only affected by being submerged in water (NW), where the null hypothesis was rejected. Without the submerged in water and wetting and drying (ND) values in an ANOVA statistical test, the moduli of elasticity for (NN, NH, NT) all match within 63.5% which is much higher than the required alpha value of 5%. The submerged in water test reduced the mean modulus of elasticity by 51.7%. For samples without reinforcement subjected to fungal treatments, being subjected for two years to fungi (NF2) resulted in the largest decrease, 24% in MOE from the unreinforced NN. For the hessian-reinforced samples subjected to moisture treatments, the submerged in water (HW) and wetting and drying (HD) displayed the greatest reduction in MOE, but freeze-thaw (HT) testing also reduced MOE by 28.0%. With the two year fungal exposure samples excluded, samples exposed to the historic fungal fibres all accepted the null hypothesis for the ANOVA tests and student t-tests when comparing conditions for each reinforcement location. When the two year fungal samples are included, the null hypothesis is rejected for both hessian reinforcement locations combined, however when separated into the two different reinforcement locations, AN, AF, AFf and AF2 reject the null hypothesis but BN, BF, BFf and BF2 narrowly accept the null hypothesis. The glass-reinforced fibrous plaster samples were negatively affected by being submerged in water (GW, 37.7% decrease), although the mean MOE increased by 68% for the 100% humidity test (GH).

Table 3 - Matrix of flexural samples T-test results for MS, LOP, MOE and FE, to demonstrate the variation in the flexural tests between two sets of samples. Green indicates acceptance of the null hypothesis (>0.05); therefore these two data sets are similar, and grey rejection of the null hypothesis (<0.05) which indicates significant difference between the two data sets. Note that MS and LOP are the same for specimens with no fibres. Values are presented to three significant figures.

MAXIMUM STRESS (MS)

MS - NO FIBRES/ MOISTURE TREATMENTS

	NN	NH	NW	ND	NT
NN	-	0.540	0.000	0.000	0.912
NH	-	-	0.000	0.000	0.492
NW	-	-	-	0.000	0.000
ND	-	-	-	-	0.000
NT	-	-	-	-	-

MS - NO FIBRES/ FUNGI TREATMENTS

	NN	NF	NFf	NF2
NN	-	0.823	0.067	0.000
NF	-	-	0.000	0.088
NFf	-	-	-	0.000
NF2	-	-	-	-

MS - GLASS FIBRES/ MOISTURE TREATMENTS

	GN	GH	GW	GD	GT
GN	-	0.000	0.000	0.000	0.013
GH	-	-	0.000	0.016	0.033
GW	-	-	-	0.024	0.000
GD	-	-	-	-	0.000
GT	-	-	-	-	-

MS - HESSIAN FIBRES/ MOISTURE TREATMENTS

	HN	HH	HW	HD	HT
HN	-	0.140	0.002	0.000	0.054
HH	-	-	0.208	0.033	0.004
HW	-	-	-	0.183	0.000
HD	-	-	-	-	0.000
HT	-	-	-	-	-

MS - HESSIAN FIBRES/ FUNGI TREATMENTS

	AN	AF	AFf	AF2	BN	BF	BFf	BF2
AN	-	0.051	0.000	0.004	0.803	0.000	0.022	0.139
AF	-	-	0.000	0.000	0.069	0.139	0.002	0.006
AFf	-	-	-	0.000	0.000	0.000	0.000	0.000
AF2	-	-	-	-	0.002	0.000	0.335	0.259
BN	-	-	-	-	-	0.001	0.012	0.094
BF	-	-	-	-	-	-	0.000	0.000
BFf	-	-	-	-	-	-	-	0.682
BF2	-	-	-	-	-	-	-	-

LIMIT OF PLASTICITY (LOP)

LOP - NO FIBRES/ MOISTURE TREATMENTS

	NN	NH	NW	ND	NT
NN	-	0.540	0.000	0.000	0.912
NH	-	-	0.000	0.000	0.492
NW	-	-	-	0.000	0.000
ND	-	-	-	-	0.000
NT	-	-	-	-	-

LOP - NO FIBRES/ FUNGI TREATMENTS

	NN	NF	NFf	NF2
NN	-	0.823	0.067	0.000
NF	-	-	0.000	0.088
NFf	-	-	-	0.000
NF2	-	-	-	-

LOP - GLASS FIBRES/ MOISTURE TREATMENTS

	GN	GH	GW	GD	GT
GN	-	0.001	0.000	0.000	0.020
GH	-	-	0.000	0.005	0.736
GW	-	-	-	0.006	0.000
GD	-	-	-	-	0.065
GT	-	-	-	-	-

LOP - HESSIAN FIBRES/ MOISTURE TREATMENTS

	HN	HH	HW	HD	HT
HN	-	0.012	0.000	0.000	0.002
HH	-	-	0.000	0.001	0.139
HW	-	-	-	0.276	0.037
HD	-	-	-	-	0.187
HT	-	-	-	-	-

LOP - HESSIAN FIBRES/ FUNGI TREATMENTS

	AN	AF	AFf	AF2	BN	BF	BFf	BF2
AN	-	0.156	0.000	0.004	0.000	0.000	0.000	0.000
AF	-	-	0.000	0.030	0.000	0.000	0.000	0.000
AFf	-	-	-	0.004	0.091	0.139	0.007	0.738
AF2	-	-	-	-	0.075	0.013	0.000	0.000
BN	-	-	-	-	-	0.555	0.000	0.008
BF	-	-	-	-	-	-	0.000	0.005
BFf	-	-	-	-	-	-	-	0.001
BF2	-	-	-	-	-	-	-	-

MODULUS OF ELASTICITY (MOE)

MOE - NO FIBRES/ MOISTURE TREATMENTS

	NN	NH	NW	ND	NT
NN	-	0.330	0.000	0.053	0.276
NH	-	-	0.000	0.000	0.964
NW	-	-	-	0.001	0.000
ND	-	-	-	-	0.000
NT	-	-	-	-	-

MOE - NO FIBRES/ FUNGI TREATMENTS

	NN	NF	NFf	NF2
NN	-	0.848	0.000	0.335
NF	-	-	0.004	0.523
NFf	-	-	-	0.014
NF2	-	-	-	-

MOE - GLASS FIBRES/ MOISTURE TREATMENTS

	GN	GH	GW	GD	GT
GN	-	0.000	0.000	0.164	0.336
GH	-	-	0.000	0.000	0.000
GW	-	-	-	0.000	0.000
GD	-	-	-	-	0.896
GT	-	-	-	-	-

MOE - HESSIAN FIBRES/ MOISTURE TREATMENTS

	HN	HH	HW	HD	HT
HN	-	0.093	0.000	0.000	0.026
HH	-	-	0.000	0.000	0.179
HW	-	-	-	0.937	0.078
HD	-	-	-	-	0.064
HT	-	-	-	-	-

MOE - HESSIAN FIBRES/ FUNGI TREATMENTS

	AN	AF	AFf	AF2	BN	BF	BFf	BF2
AN	-	0.078	0.001	0.857	0.322	0.154	0.003	0.030
AF	-	-	0.000	0.052	0.012	0.008	0.000	0.002
AFf	-	-	-	0.001	0.012	0.113	0.454	0.664
AF2	-	-	-	-	0.401	0.190	0.004	0.038
BN	-	-	-	-	-	0.545	0.015	0.134
BF	-	-	-	-	-	-	0.065	0.369
BFf	-	-	-	-	-	-	-	0.333
BF2	-	-	-	-	-	-	-	-

FRACTURE ENERGY (FE)

FE - NO FIBRES/ MOISTURE TREATMENTS

	NN	NH	NW	ND	NT
NN	-	0.263	0.000	0.000	0.417
NH	-	-	0.001	0.000	0.663
NW	-	-	-	0.287	0.000
ND	-	-	-	-	0.000
NT	-	-	-	-	-

FE - NO FIBRES/ FUNGI TREATMENTS

	NN	NF	NFf	NF2
NN	-	0.852	0.003	0.283
NF	-	-	0.000	0.139
NFf	-	-	-	0.017
NF2	-	-	-	-

FE - GLASS FIBRES/ MOISTURE TREATMENTS

	GN	GH	GW	GD	GT
GN	-	0.000	0.000	0.000	0.093
GH	-	-	0.000	0.001	0.003
GW	-	-	-	0.115	0.000
GD	-	-	-	-	0.000
GT	-	-	-	-	-

FE - HESSIAN FIBRES/ MOISTURE TREATMENTS

	HN	HH	HW	HD	HT
HN	-	0.434	0.677	0.000	0.047
HH	-	-	0.588	0.003	0.006
HW	-	-	-	0.000	0.001
HD	-	-	-	-	0.000
HT	-	-	-	-	-

FE - HESSIAN FIBRES/ FUNGI TREATMENTS

	AN	AF	AFf	AF2	BN	BF	BFf	BF2
AN	-	0.014	0.000	0.795	0.042	0.000	0.000	0.251
AF	-	-	0.000	0.004	0.229	0.220	0.000	0.062
AFf	-	-	-	0.000	0.000	0.000	0.000	0.000
AF2	-	-	-	-	0.004	0.000	0.000	0.081
BN	-	-	-	-	-	0.002	0.000	0.214
BF	-	-	-	-	-	-	0.000	0.000
BFf	-	-	-	-	-	-	-	0.000
BF2	-	-	-	-	-	-	-	-

3.1.4 **Fracture Energy (FE)**

Compared to the plaster samples with no reinforcement, the fracture energy (FE) for the plaster samples submerged in water (NW) and wetting and drying (ND) tests decreased, with the null hypothesis being rejected. Hessian-reinforced plaster subjected to moisture treatments was affected by the wetting and drying (HD) and freeze-thaw conditions (NT). For the wetting and drying test, FE decreased by 27.4%, conversely it increased for the freeze-thaw test by 19%. For the samples exposed to the historic fibres, the hessian-reinforced samples rejected the null hypothesis for the ANOVA tests, as indeed did the unreinforced plaster-only samples subjected to fungal treatments. For both locations of hessian reinforcement without any food source present, FE increased significantly enough for the null hypothesis to be rejected (49.3% increase for 1mm away from bottom of sample and 30% increase for almost at the bottom of the sample). Hessian fibre samples subjected to historic fungi for two years displayed a significant reduction in FE, with ANOVA analysis showing AF2 reducing by 87.2% in comparison to AN, and BF2 reducing by 74.7% in comparison to BN; therefore, the two year treatment showed the greatest impact upon deteriorating the hessian fibres to impact FE. Glass fibre samples had the biggest decrease in FE for 100% humidity (GH), submerged in water (GW) and wetting and drying (GD) tests and the null hypothesis was again rejected.

To summarise the flexural tests, overall the conditions which affected the samples to the greatest extent and consequently causing a deterioration in the mechanical properties were:
Moisture treatments:

- being submerged in water
- wetting and drying and

Fungal treatments:

- exposure to the historic fungi
- subjected to fungus for two years with a food source for the fungal treatments – this in particular showed a very significant negative impact upon FE.

3.2 **Scanning Electron Microscopy (SEM)**

After having been exposed to the respective moisture and fungal-related environmental conditions, by observation black-coloured fungal growth was evident on the sample specimens in this study. This was most notable particularly on the 100% humidity samples for the moisture treated conditions and samples which had been exposed to fungi growing on the historic hessian fibres, especially where the fungi had a food source and the specimens were left in a covered box for two years. SEM images of samples HH (100% RH) and BFf (samples exposed to fungi with a food source) can be seen in Figure 7.

In contrast with the gypsum matrix and hessian fibre SEM images of newly manufactured samples not subjected to moisture or fungal-related treatments illustrated in [8], which showed no visual indications of degradation or fungal growth, entangled masses of hyphae (mycelium) were observed in Figure 7*a* and *b* covering the hessian and gypsum plaster matrix. No fungal spores from historic fibrous plaster samples were explicitly introduced in the 100% RH HH specimens., Hence, the fungus is able to grow on the fibrous plaster samples, even when not directly exposed to fungus on historic samples and fungi are able to grow on the gypsum plaster matrix as well as hessian fibres. Some hyphae are broken, exposing the hollow interior of the tubular structure; in addition, exterior surface nodules are visible showing a coarser exterior hyphae surface. Fungal spores are not evident in this image though, suggesting the level of fungal growth and expansion would be lower.

Figure 7*c* shows an array of fungal spores on a BFf test sample, growing on the surface of the angular gypsum crystals and 5*d* reveals a closer look at the spores and hyphae. The malt extract food source is shown in 5*e* and 5*f,* being invaded by the fungus - both spores and hyphae are seen to be inside the hollowed-out shells of the food source, with hyphae growing from the food source.

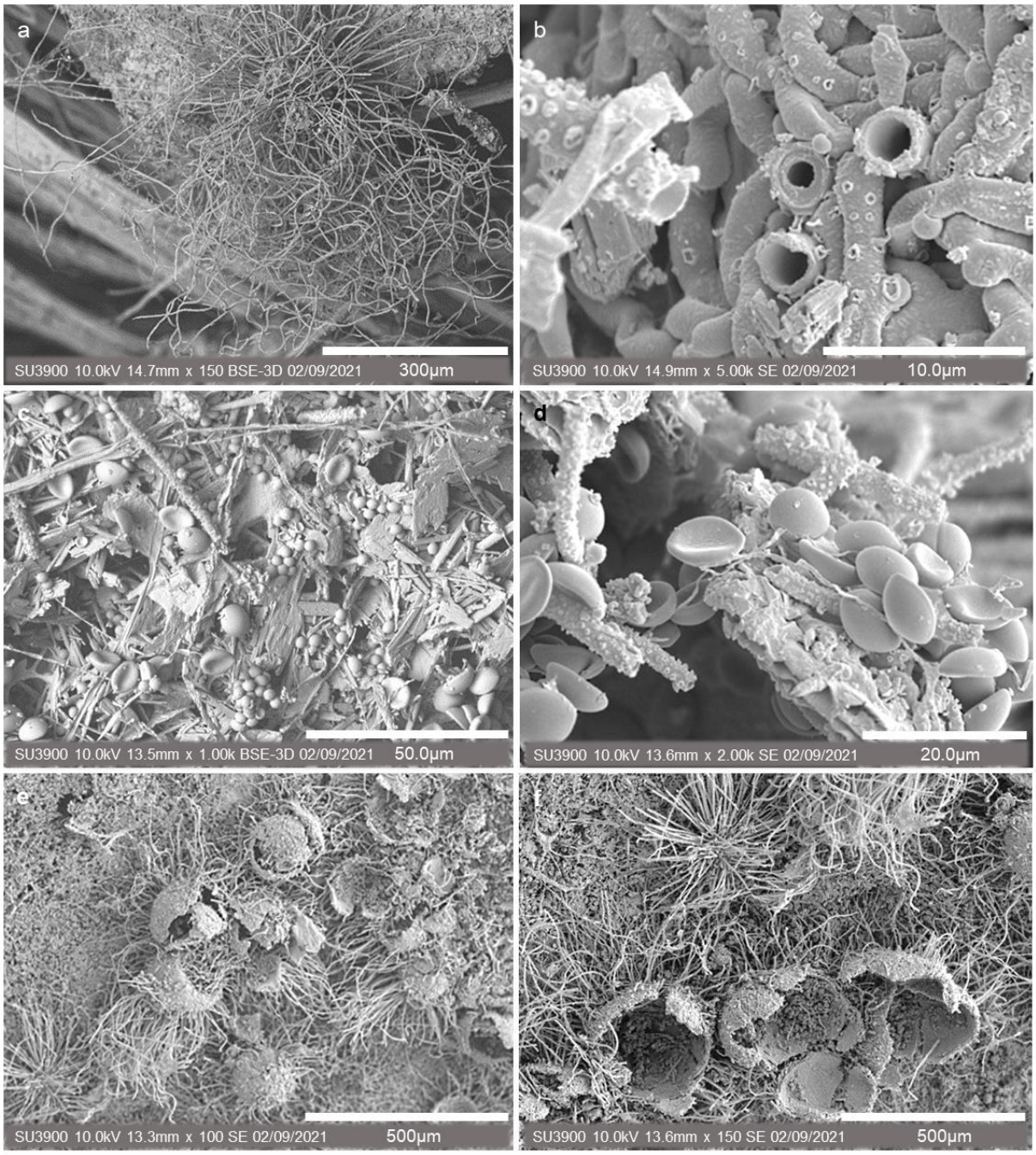

Figure 7 – SEM imaging showing fungal growth on test samples, a) x150 magnification of a sample in condition HH showing fungal hyphae, b) x5000 magnification of the hyphae in the HH sample, c) x1000 magnification of fungal spores in a sample subjected to the condition BFf, d) BFf spores observed at x2000 magnification, e) Fungal hyphae growing out of the hollow shells of the food source in the BFf sample and f) x150 magnification of hyphae and food source shells in the BFf sample.

3.3 DNA Fungal identification

Upon completion of SEM tests, DNA sequencing took place on the samples to accurately identify the fungus type. Using BLAST paired up with the DNA sequences, which were found from the samples collected on the agar plates, the closest matches to the fungi on the database were *Penicillium rubens* and *Chaetomium globosum*. These were the only two fungal species isolated from the inside of the samples and the match certainty for these specific fungus types was high; manual assignment of species was based on both sequence similarity to the top hit in the database and on the exclusivity of that hit. For example, a sequence would be considered to represent a species if it had greater than 99% similarity to a named representative of 'that species in the database, but not if it also had equal similarity to another named taxon. With *P. rubens and C. globosum* identified, specimens of the fungi were grown in sealed petri dishes in an ambient temperature of 20°C for a period of three weeks (with food source particles included within the petri-dish to promote growth) and the ensuing *P. rubens* and *C. globosum* mould growth formed part of the FTIR experimentation and analysis.

3.4 Fourier Transform Infrared Spectroscopy

The FTIR results for the hessian fibres obtained from the flexural samples are shown in Figure 8, with part *a* plotting R_1 verses R_2 for all samples tested to identify the formation of distinct clusters for each treatment category – with multiple hessian fibre specimens from one sample in each treatment category tested. Part *b* plots the mean R_1 verses R_2 values for each treatment category, part *c* shows the mean R_1 values with the error bars denoting the standard deviation and part *d* showing the mean R_2 values also with the error bars denoting standard deviation. Sample conditions which are lower-left in the part *a* and *b* charts are dominated by fungal treatment, with samples subjected to two years (AF2 and BF2 series) with defined clusters in part *a* showing the lowest R_1 and R_2 values. Progressing along the axes, these are followed by BFf and AFf, with the 100% humidity (HH) then following for the moisture treatment samples and ultimately the other moisture treatments and no-treatment samples rightmost. 'New hessian' (NH) was not part of a fibrous plaster flexural sample, but new hessian fibres tested for comparison – this group is most distinct at the top of parts *a* and *b*.

Figure 9 shows the FTIR spectra for the grown *P.rubens* and *C. globosum* moulds, along with the food source and examples of FTIR spectra for the hessian fibres, to show the differences observed in spectra peaks. In part *a*, the fungal treatment category 'A' is shown, with AN (no treatment) and AF2 (exposed to fungi for two years), with fungal growth visually evident on the flexural samples. Treatment category A was chosen to visualise as this represents a wide range of results both in flexural strength and position on the $R_1 – R_2$ plots, with AN performing well in strength tests ranging through to AF2 performing less well. In part *b*, pure *P. rubens* mould is shown, along with new hessian fibres and the new hessian fibres brushed with *P. rubens*, to represent an in-situ scenario in a period building where fungi might be present on partially exposed hessian fibres. In part *c*, pure *C. globosum* is shown along with new hessian (untreated) and new hessian brushed with *C. globosum*. The wavelengths used for the peak ratios 1105, 1735 and 2900 cm^{-1} are indicated. At wavelength 1105 cm^{-1}, small shoulder peaks in transmission are more evident for the new hessian fibre samples than on the pure mould spectra. With the 'A' treatment category samples, there are pronounced peaks at 1105 cm^{-1}, with a reduction in peak intensity for AF2 in comparison to AN. At wavelength 1735 cm^{-1}, the new hessian samples and hessian brushed in mould show small shoulder peaks which are not evident on the pure mould samples. The 'A' treatment category hessian shows small peaks which are quite uniform for the different samples. At 2900 cm^{-1}, the 'A' treatment category samples show a small peak, with variation in the AF2 spectra between 1735 and 2900 cm^{-1}

and from 2900 to 4000 cm^{-1} in comparison to AN. Small peaks are in evidence with the new hessian and new hessian brushed with mould; no peaks are evident with pure mould samples.

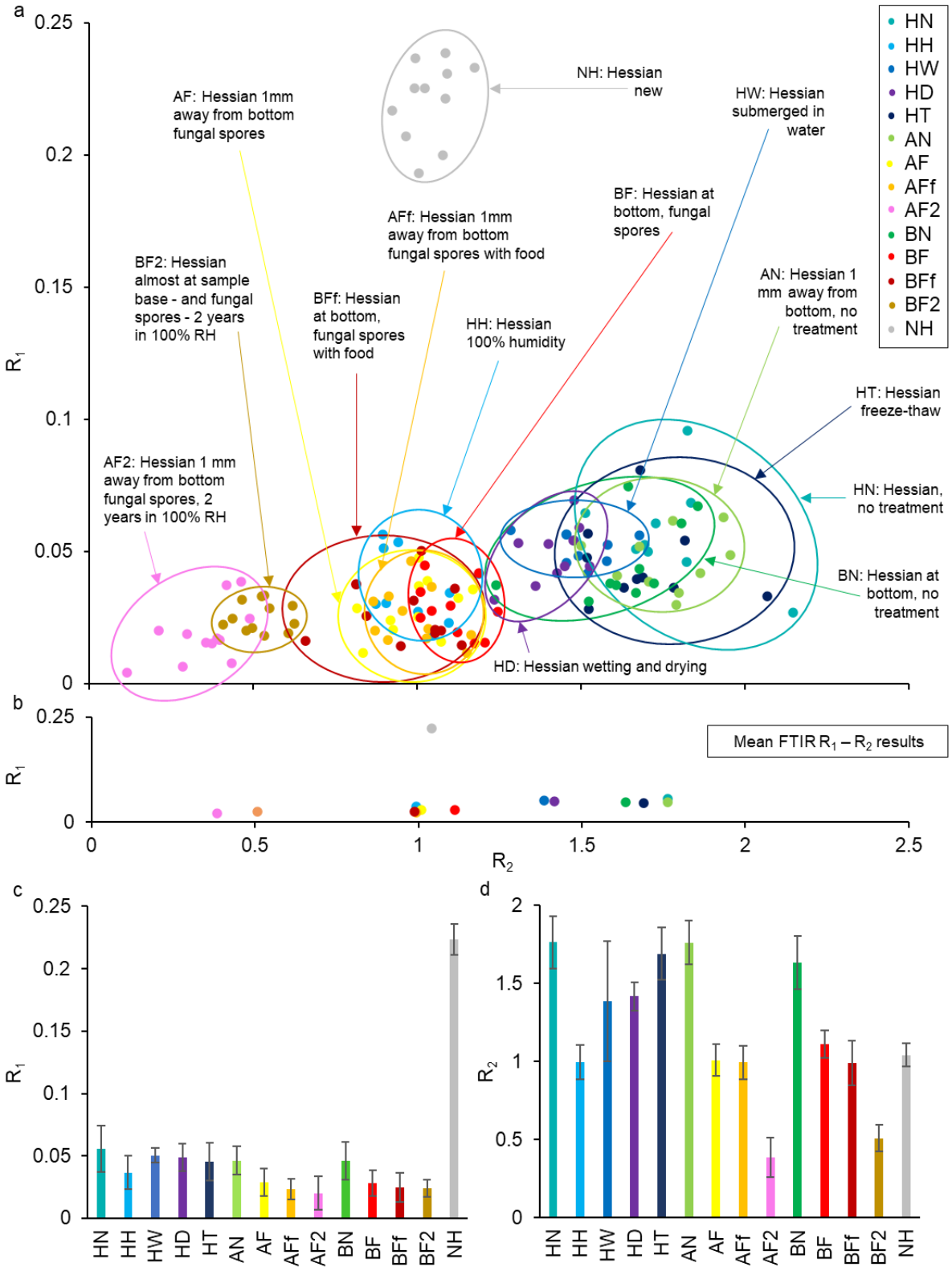

Figure 8 - FTIR peak ratios for hessian fibres taken from the range of moisture and fungal treatment samples a) R_1 and R_2 plotted against each other – at least ten specimens of hessian fibre from one sample from each sample set, b) Mean R_1 and R_2 values from the sample sets, c) Mean R_1 values for each sample set with the standard deviation for each sample set, d) Mean R_2 values with the standard deviation for each sample set.

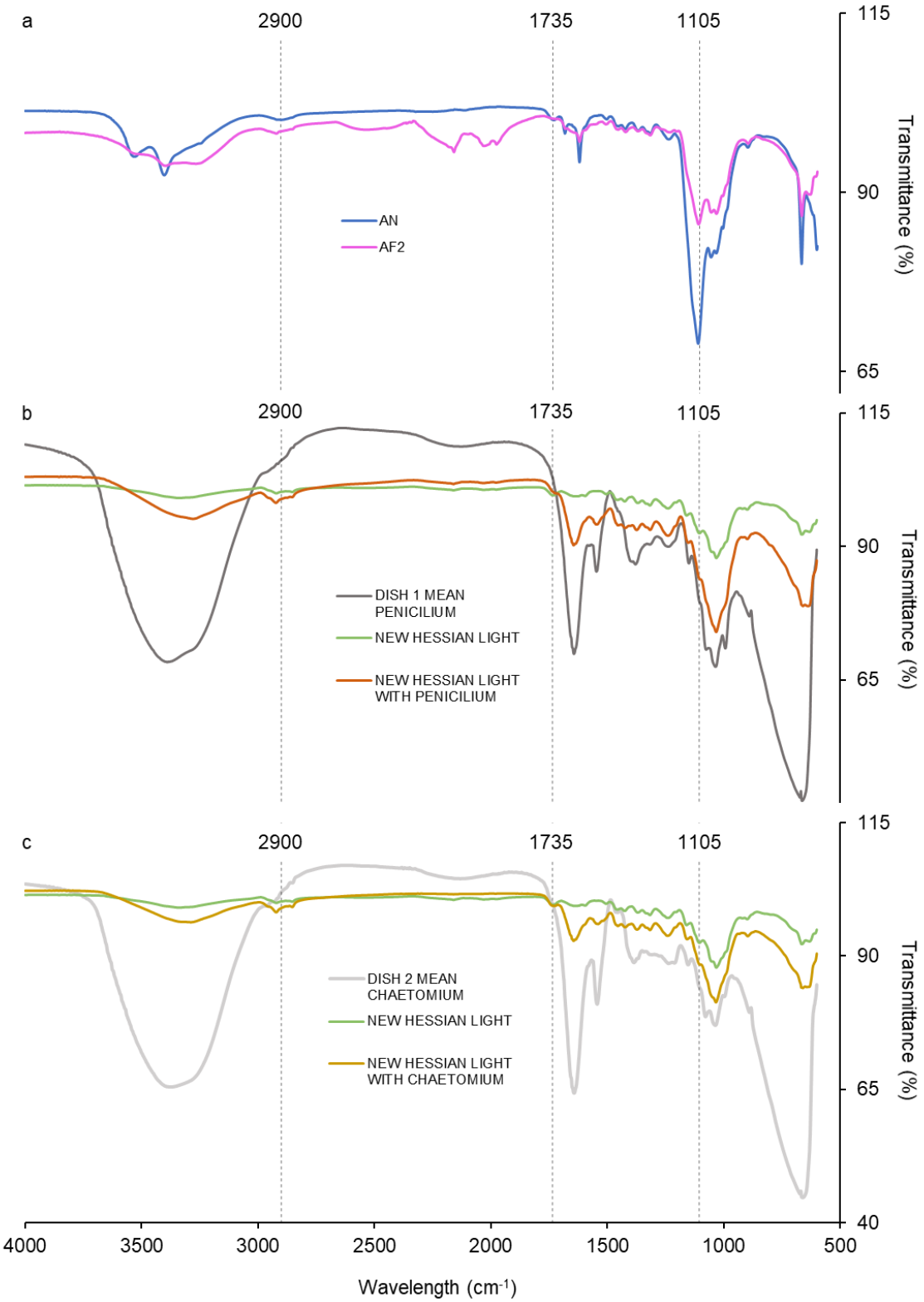

Figure 9 – Comparison of FTIR spectra for Penicillium and Chaetomium moulds along with the food source, hessian fibres from the 'A' range of fungal treatments, new untreated hessian and new hessian brushed in mould to represent an in-situ scenario in a period building of fungi present on fibres. a) Hessian from flexural samples in the 'A' treatment range with AN (no treatment), AF2 (exposed to fungi for two years). b) Pure Penicillium rubens, new hessian and new hessian brushed with P.rubens. c) Pure Chaetomium globosum, new hessian and new hessian brushed with C. globosum. The wavelengths at 1105, 1735 and 2900 used for the R_1 and R_2 peak ratios are indicated by dashed vertical lines.

4 Discussion

Different mechanisms that affect and degrade fibrous plaster can be evaluated by comparison of the results from the mechanical test data, FTIR results and R_1 versus R_2 plots derived from the FTIR data. The results of three-point bending tests reflect the pre-conditioning by submersion in water, wetting and drying, exposure to fungi with food, and exposure to fungi with food for two years. Unreinforced gypsum was affected by the treatment conditions as well as reinforced plaster, which emphasises the observation that gypsum itself is also vulnerable to experiencing degradation and it is not just an issue for reinforcing hessian fibres. The FTIR data shows defined 'clusters' corresponding with treatment conditions and this, in conjunction with the flexural test results, demonstrates the potential of using FTIR peak ratios for identifying degradation mechanisms of hessian fibres in fibrous plaster and the extent to which the mechanism has caused degradation.

There is a distinction between moisture conditions and fungal conditions, with the 100% humidity test in the moisture conditions being closest to the fungal conditions in terms of the FTIR R_1 versus R_2 charts in Figure 8. The submerged in water and wetting and drying tests are situated around the median of the sets, so are performing less well than the untreated samples as would be expected from reviewing the flexural data results. There is also less variance in submerged in water and wetting and drying tests data in the FTIR data, so the fibres are affected to approximately the same degree each time.

Moisture has shown to decrease the strength of natural fibres such as flax by saturation following Fickian diffusion behaviour. Natural fibres absorb more water than glass fibres which is expected due to the material types; the saturation leads to water ageing of the fibres [17]. For the submerged in water tests and wetting and drying, this saturation, and therefore loss of strength is likely occurring. *Penicillium rubens* is a fungus commonly found indoors [39] and *Chaetomium globosum* is usually found both indoors and outdoors, so it was not surprising for them to be present on the samples tested. As slow growing species, both types may not be damagingly invasive in the short-term, but there could be potential for degradation over a long period of time. For *P. rubens* to grow quickly, there is a need for a relative humidity level above 90% [40]. Indeed, the 100% humidity treatment and fungal treatment test specimens have black mould visible (Figure 6); The photographs are of the most visibly affected samples from the fungal attack as well as those with no reinforcement to demonstrate the difference.

It can be observed that the FTIR peak ratio approach displays clearly defined clusters of data points for the different fungus and moisture treatments. Working from the left of the R_2 x-axis and moving to the right, it can be observed that fungal treated samples are placed furthermost left, followed by the moisture categories of wetting and drying, submerged in water and 100% RH and finally the untreated samples and freeze-thaw to the furthermost right. Comparing these FTIR ratio results to the flexural results, it can be broadly reasoned that the most extreme case is the two-year fungal category, followed by the other fungal categories and the moisture categories wetting and drying, submerged in water and 100% RH and then finally the least onerous, along with no treatment at all, being freeze-thaw.

With the use of peak ratios in this study, it was aimed to demonstrate that the changes in R values observed are due to fibre degradation, rather than just confirmation of the presence or type of fungi. The FTIR spectra show that 'pure' *P. rubens* and *C. globosum* mould is distinct from hessian fibres, with the fibres containing mould applied to the surface using a fine brush (simulating a more realistic in-situ/roof space occurrence with fungi on hessian) showing spectra more in line with hessian fibres non-brushed rather than pure mould. For example, the intense peaks at 1105 cm^{-1} (C-O-C bonds, representing cellulose content) in the fungal

737 treatment specimens ‘A’ in Figure 9*a* are not evident in the mould or new (untreated) Hessian
738 spectra in parts *b* and *c*. Therefore, it can be postulated that the FTIR peak-ratios approach
739 can demonstrate a degree of identification of how different fungal and moisture treatments
740 affect hessian fibres.
741
742 The C-O-C bond shows greater absorption at 1105 cm^{-1} in the AN specimens than in the AF2
743 specimens and it is the bond which shows the most notable variation from new hessian. It is
744 reasoned the degradation of cellulose (and possible change in cellulose structure due to fungal
745 attack) in the specimens subjected to fungi for two years contributed to the reduced
746 performance in strength. Penicillium species are capable of secreting multi-enzyme systems
747 capable of degrading cellulose [41] and breaking glycosidic bonds resulting in hydrolysis and
748 the formation of sugar molecules [42]. Hulleman et al. 1994 state that when cellulose changes
749 between different degrees of crystalline to amorphous structure, spectra peaks can alter at
750 numerous wavelengths including 1105 cm^{-1} (due to anti-symmetric in-phase ring stretching at
751 that wavelength) [43]. The difference in peaks between the ‘A’ treatment samples, new hessian
752 and mould can be reasoned to demonstrate degradation of the cellulose in aged hessian due
753 to the prolonged fungal treatment, resulting in a loss of strength. At 1735 cm^{-1}, the C=O bond
754 showing Pectin does not show a reduction in absorption from AN to AF2 and is not visually
755 notably different to new hessian. New hessian and untreated AN specimens were expected to
756 differ to an extent due to AN specimens being present within a gypsum plaster matrix for the
757 duration of laboratory preparation and testing.
758
759 As discussed by Majumber et al. [27], genes associated with jute varieties affect their ability to
760 resist degradation during cultivation, which could be a reason for fungal degradation in some
761 cases. In Figure 7, hyphae, and fungal spores coat both the gypsum and jute fibres. Gypsum
762 inoculated with *P. rubens* formed mycelium and hyphae on its surface as well as germinating
763 in water [44]. This species grows readily on indoor surfaces and was found to grow in humid
764 conditions on the gypsum [25]. *C. globosum* is known to have degraded jute fibres in storage
765 conditions, which gives a strong suggestion that the fungus could be slowly affecting the
766 strength of the fibres. However, treatment of the fibres was found to reduce its growth
767 significantly [45], meaning fungal growth could be greatly reduced by using chemicals to treat
768 hessian fibres prior to incorporation into fibrous plaster as part of the manufacturing process –
769 though this would naturally introduce cost, time and resource considerations.

770 Moisture and fungal conditions for fibrous plaster degradation are linked, with moisture being
771 present and starting an ageing process (through being submerged in water or wetting and
772 drying for example), which then leads to the growth of fungus which will in turn cause further
773 degradation.

774 Historic fibrous plaster ceilings, in close proximity to external roofs, are vulnerable to water
775 leaks from either the roof or pipes located between the ceiling and the roof, with moisture
776 capable of filtering through to the plaster and hessian. Fluctuations in temperature would also
777 be greater closer to the roof which in extremely cold weather could potentially lead to the
778 freeze-thaw cycles occurring in an uninsulated, non-airtight aged roof space. According to
779 research undertaken in Denmark, the attic of a house had large temperature variations due to
780 the roof having the lowest U-value. In cold, moist outdoor temperatures, there was a higher
781 moisture content inside the roof space, so the historic fibrous plaster ceilings would be exposed
782 to moisture from the roof space above [46].
783
784 Fungal spores are also more likely to be present in these areas due to their proximity to the
785 outside elements from the roof. A roof space is not likely to be cleaned as often as a living or
786 occupied space (even though there can be walkways in the roof spaces of period buildings),
787 leading to the potential for heavy reproduction of fungal spores and food sources for the fungi

potentially building up. Interestingly, fungi are often found to attack timber building materials; considering historic fibrous plaster is often suspended from or bound to wooden battens, the presence of fungi is to be expected as wooden structures are often coated in a biofilm of micro-organisms [47].

The distinctive nature of the flexural graphs for plaster without reinforcement demonstrates its brittle nature and tendency to fail suddenly. Gypsum plaster can be modelled as a lattice structure filled with pores. The pores mean it will have a tendency to let water in which may cause problems, combined with its brittle nature, which then leads to failure problems with the gypsum plaster [48]. The unreinforced plaster during the degradation testing was clearly affected the most by being submerged in water and during wetting and drying tests. Moisture is known to increase the subcritical crack growth and creep within plaster. The needle-shaped gypsum crystals have a weak interface where water decreases the strength of the bonds by thickening the adsorbed water layers, causing crystals to slide over each other [49]. For the samples which were submerged in water, the pores between the gypsum crystals would be fully saturated, leading to the adsorbed water layer becoming over-saturated. Once removed from the water, the pores would still contain the water, which would act as a lubricant to the gypsum particles when the load was applied.

Material dissolution could be the other potential cause of gypsum weakness, though this cause of failure is much less likely due to the studies undertaken by Reynaud et al. [49]; tests were completed to determine if lubrication or dissolution was the issue by using water and ethanol for comparison. Ethanol will not dissolve gypsum, yet when applied to the plaster, a similar graph to that of water being added presented itself, concluding the lubrication mechanism is the main issue [49]. Wetting and drying tests were the other degradation issue causing problems for all the samples, although to a lesser extent than the submerged in water tests. The drying time allows the surface water to escape, rather than having permanent porosity saturation. Water does become trapped within gypsum plaster once filling up the inner pores [50]. This trapped water then has the same effect as the samples submerged in water with the gypsum crystals sliding.

An important finding was that the unreinforced plaster was affected by the water as this suggests the plaster, as well as reinforcement, is vulnerable. The mechanism involving the saturated water layer explains the reasoning for failure of the gypsum. Originally the hessian scrim was deemed to be a potential cause of failure with the rotting or degradation of the fibres being a main concern. Stamboulis et al., 2000 discussed fibres swelling from water causing further cracks within plaster, leading to the weakening of the plaster [22]. There is still a possibility that hessian degradation is occurring within the sample, in addition to the aforementioned plaster degradation, but results of this study suggest plaster itself is also a concern. Comparing the difference between the plaster affected by moisture with and without hessian reinforcement can determine the answer; submerged in water sample sets (NW and HW) have similar LOP and MOE, but the MS and FT is much higher as expected because of the hessian reinforcement.

From this comparison, it can be concluded that a likely cause of failure in historic fibrous plaster through a moisture-related mechanism is the gypsum plaster failing, confirmed by the LOP and MOE being similar, rather than just the hessian fibres degrading. For the samples subjected to fungal treatment, the hessian 1 mm away from the bottom surface of the samples had inferior mechanical properties to specimens with hessian nearly touching the bottom surface. Hence, in flexure there seems to be no discernible benefit in situating the hessian fibre further away from the external surface of the fibrous plaster, due to the hygroscopic properties of gypsum plaster and inherent vulnerability to moisture, and fibres further from the surface being affected by absorbed and retained moisture to a greater extent than fibres closer to the surface.

It is important to remember the results of this study are based on laboratory experiments, and in real world in-situ applications each fibrous plaster ceiling is an individual creation in a unique environment. However, laboratory experiments can determine material properties and behaviour under stated conditions and contribute towards a scientific basis to the understanding of how a historic fibrous plaster element in-situ may degrade over time and the linked moisture and fungal mechanisms of degradation. The FTIR peak ratio approach demonstrates the potential for identifying the mechanisms of degradation in fibrous plaster elements displaying evidence of aged-related deterioration in real-world applications and historic buildings. Using the R_1 verses R_2 plot approach demonstrated, an FTIR-based approach may be used to analyse historic fibrous plaster specimens. Subject to the consent of building owners, an exposed fibre of in-situ hessian material suitable for FTIR may be taken for laboratory analysis and the peak ratio plot used to determine potential causes of degradation (or lack of degradation if it is in the region of the new fibres on the $R_1 – R_2$ plot). This would provide information on the conditions within the roof space and perhaps identify fungal presence. It was determined by the investigation following the Apollo Theatre collapse in 2013 that failure of the ceiling was due to ageing in the fibrous plaster material rather than direct evidence of any liquid water ingress or action [51]. Hessian wadding tie material is considered to have a finite life [51] which has been postulated as 80 years [52] – therefore degradation of the material is of prime importance. The contribution of this study to demonstrating the influence of fungi and water vapour levels will aid understanding of how vulnerable fibrous plaster is in the environments of theatres and other buildings with ageing building envelopes and high (and inconsistent) occupation levels. Many buildings containing fibrous plaster are listed and therefore protected, with the removal of material often being minimised; identifying degraded areas and harvesting very small amounts of material for analysis would promote effective restoration and conservation of historic and culturally significant buildings.

5 Conclusions

This study has demonstrated through a programme of laboratory tests – flexural, SEM, DNA and FTIR - that moisture ingress and fungal attack have a detrimental effect on the mechanical properties of fibrous plaster and the results contribute to evidence that moisture and fungi are major causes of degradation. While experiments took place in a controlled laboratory environment and fibrous plaster elements are typically installed in historic buildings, each of which may be considered a prototype, this study provides a scientific base to add to the empirical understanding of fibrous plaster and its performance and behaviour by providing:

- Quantification of the effects of a range of moisture and fungal treatments on the mechanical properties of fibrous plaster
- The identification of fungi present on historic fibrous plaster samples
- The use of FTIR and an adapted peak ratio method to identify and analyse the effects of fungi and mechanisms of degradation on hessian fibres, with the breaking of cellulose glycosidic bonds within hessian as a result of fungal exposure identified as a potent degradation mechanism. Test specimens subjected to different moisture and fungal treatments can be identified by defined clusters on an FTIR peak ratio plot and compared with flexural strength results.

This study highlights the importance of fibrous plaster ceilings being surveyed and monitored for signs of moisture ingress or fungal degradation to prevent potentially dangerous failures from happening in the future. Evidence of moisture ingress or fungal damage needs to be addressed and a very small sample of fibre could be harvested in-situ and taken for laboratory analysis. Application of the FTIR-based approach in this study could determine the degradation mechanism and promote efficient restoration and conservation.

From the research and data analysis in this study, it can be concluded that the highest risks posed to the properties and behaviour of historic fibrous plaster with the moisture treatments are water submersion (which is particularly detrimental to the plaster matrix) and repeated wetting and drying cycles, plus fungal attack with a food source and prolonged exposure over a period of years. Results – in particular the reduction of flexural strength - suggesting attack from fungi over a long time period as being the most onerous degradation mechanism of all for fibrous plaster.

6 Acknowledgements

The authors gratefully acknowledge the funding of the Leverhulme Trust, grant number RPG-2021-147.

The authors additionally thank the following for support and guidance:

The entire management and fibrous plaster teams at Hayles and Howe Ornamental Plasterwork and Scagliola, Bristol, United Kingdom for their time, resources and manufacture of the flexural test samples, plus the donation of historic fibrous plaster samples for laboratory analysis.

Locker and Riley artisans in plaster, South Woodham Ferrers, Chelmsford, United Kingdom for donating historic fibrous plaster samples.

Richard Ireland (historic decorative plaster and paint consultant, Plaster and Paint, United Kingdom).

Scott Brookes (structural engineering consultant, Ramboll, United Kingdom).

With thanks to the following: Berrak Balci (Researcher – flexural tests, Department of Architecture and Civil Engineering, University of Bath), William Bazeley and Neil Price (Technical support – flexural tests, Department of Architecture and Civil Engineering, University of Bath) and Philip J. Fletcher (SEM imaging and FTIR testing guidance and input, Department of MC^2, University of Bath).

The FTIR and Flexural test data for moisture and fungal degradation samples supporting this manuscript are available from the Dataset for the results of fibrous plaster tests, University of Bath Research Data Archive, https://doi.org/10.15125/BATH-01213.

References

[1] J. Stewart *et al.*, “Historic Fibrous Plaster in the UK. Guidance on its Care and Management,” *Hist. Engl.*, 2019, [Online]. Available: https://historicengland.org.uk/images-books/publications/historic-fibrous-plaster/heag269-historic-fibrous-plaster/.

[2] S. Brookes, K. Clark, R. Frostick, R. Ireland, and L. Randall, “The Plaster Ceilings of Buckingham Palace and Windsor Castle: Their Construction, Condition and Conservation,” in *12th International Conference on Structural Analysis of Historical Constructions*, 2020, doi: 10.23967/sahc.2021.293.

[3] BBC, “Apollo Theatre - Ceiling collapses during show in London,” *BBC*, 2013. https://www.bbc.co.uk/news/uk-england-25458009 (accessed Jun. 12, 2022).

[4] A. France, “Savoy ballroom ceiling collapses, showering black-tie auction guests with debris,” *Evening Standard*, 2019. https://www.standard.co.uk/news/london/savoy-ballroom-ceiling-collapses-showering-blacktie-auction-guests-with-debris-a4082701.html (accessed Jun. 12, 2022).

[5] S. Brookes, “Historic plaster ceilings. Part 1: Development and causes of failure,” *Struct. Eng.*, vol. 99, no. 3, pp. 20–24, 2021.

[6] ABTT, “ABTT Guidance Note 20 May 2015 Advice to Theatre Owners and Managers regarding Suspended Fibrous Plaster Ceilings ; Survey , Certification , Record Keeping etc .,” no. May, 2015.

[7] E. M. Payne, “The Conservation of Plaster Casts in the Nineteenth Century,” *Stud. Conserv.*, vol. 65, no. 1, pp. 37–58, 2020, doi: 10.1080/00393630.2019.1610845.

[8] S. A. Ngah, B. Dams, M. P. Ansell, J. Stewart, R. Hempstead, and R. J. Ball, “Structural performance of fibrous plaster. Part 1: Physical and mechanical properties of hessian and glass fibre reinforced gypsum composites,” *Constr. Build. Mater.*, vol. 120396, 2020.

[9] N. B. Singh and B. Middendorf, “Calcium sulphate hemihydrate hydration leading to gypsum crystallization,” *Prog. Cryst. Growth Charact. Mater.*, vol. 53, no. 1, pp. 57–77, 2007, doi: 10.1016/j.pcrysgrow.2007.01.002.

[10] R. Jia, Q. Wang, and P. Feng, “A comprehensive overview of fibre-reinforced gypsum-based composites (FRGCs) in the construction field,” *Compos. Part B Eng.*, vol. 205, no. November 2020, p. 108540, 2021, doi: 10.1016/j.compositesb.2020.108540.

[11] R. Ireland, “Investigation and assessment of decorative plaster ceilings,” *J. Build. Surv. Apprais. Valuat.*, vol. 9, no. 3, pp. 228–245, 2020.

[12] S. Brookes, “Historic plaster ceilings. Part 2: Survey, assessment and methods of conservation,” *Struct. Eng.*, vol. 99, no. 4, pp. 30–33, 2021.

[13] C. H. Lee, A. Khalina, S. H. Lee, and M. Liu, “A Comprehensive Review on Bast Fibre Retting Process for Optimal Performance in Fibre-Reinforced Polymer Composites,” *Adv. Mater. Sci. Eng.*, vol. 2020, 2020, doi: 10.1155/2020/6074063.

[14] H. Yu and C. Yu, “Influence of various retting methods on properties of kenaf fiber,” *J. Text. Inst.*, vol. 101, no. 5, pp. 452–456, 2010, doi: 10.1080/00405000802472564.

[15] S. Follner, A. Wolter, K. Helming, C. Silber, H. Bartels, and H. Follner, “On the real structure of gypsum crystals,” *Cryst. Res. Technol.*, vol. 37, no. 2–3, pp. 207–218, 2002, doi: 10.1002/1521-4079(200202)37:2/3<207::AID-CRAT207>3.0.CO;2-L.

[16] A. L. Lebedev, “Kinetics of gypsum dissolution in water,” *Geochemistry Int.*, vol. 53, no. 9, pp. 811–824, 2015, doi: 10.1134/S0016702915070058.

[17] M. Assarar, D. Scida, A. El Mahi, C. Poilâne, and R. Ayad, “Influence of water ageing on mechanical properties and damage events of two reinforced composite materials: Flax-fibres and glass-fibres,” *Mater. Des.*, vol. 32, no. 2, pp. 788–795, 2011, doi: 10.1016/j.matdes.2010.07.024.

[18] P. Garside and P. Wyeth, “Identification of cellulosic fibres by FTIR spectroscopy: Differentiation of flax and hemp by polarized ATR FTIR,” *Stud. Conserv.*, vol. 51, no. 3, pp. 205–211, 2003, doi: 10.1179/sic.2006.51.3.205.

[19] M. Nath, F. T. Chowdhury, S. Ahmed, A. Das, M. R. Islam, and H. Khan, “Value addition to jute: assessing the effect of artificial reduction of lignin on jute diversification,” *Heliyon*, vol. 7, no. 3, 2021, doi: 10.1016/j.heliyon.2021.e06353.

[20] N. Graupner, “Application of lignin as natural adhesion promoter in cotton fibre-reinforced poly(lactic acid) (PLA) composites,” *J. Mater. Sci.*, vol. 43, no. 15, pp. 5222–5229, 2008, doi: 10.1007/s10853-008-2762-3.

[21] C. P. Macmillan and H. Birke, “Lignin Deposition in Cotton Cells ? Where is the lignin?,” *J. Plant Biochem. Physiol.*, vol. 1, no. 2, pp. 2–5, 2016, doi: 10.4172/2329-9029.1000e106.

[22] A. Stamboulis, C. A. Baillie, S. K. Garkhail, H. G. H. Van Melick, and T. Peijs, “Environmental durability of flax fibres and their composites based on polypropylene matrix,” *Appl. Compos. Mater.*, vol. 7, no. 5–6, pp. 273–294, 2000, doi: 10.1023/A:1026581922221.

[23] G. M. Gadd, “Geomicrobiology of the built environment,” *Nat. Microbiol.*, vol. 2, no. March, 2017, doi: 10.1038/nmicrobiol.2016.275.

[24] P. Ryparová, M. Kostelecká, and J. Tywoniak, “Biodegradation of Mineral and Silicone Plasters and Its Comparison,” *IOP Conf. Ser. Earth Environ. Sci.*, vol. 290, no. 1, 2019, doi: 10.1088/1755-1315/290/1/012030.

[25] P. Ruijten, H. P. Huinink, and O. C. G. Adan, “Hyphal growth of Penicillium rubens in changing relative humidity,” *Appl. Microbiol. Biotechnol.*, vol. 105, no. 12, pp. 5159–5171, 2021, doi: 10.1007/s00253-021-11343-6.

[26] D. Ding, T. Yu, and Y. Li, “Biodegradation of jute/poly(lactic acid) composites by fungi,” *Sci. China Technol. Sci.*, vol. 61, no. 11, pp. 1705–1712, 2018, doi: 10.1007/s11431-017-9215-7.

[27] S. Majumder, K. Datta, C. Sarkar, S. C. Saha, and S. K. Datta, “The development of macrophomina phaseolina (Fungus) resistant and glufosinate (herbicide) tolerant transgenic jute,” *Front. Plant Sci.*, vol. 9, no. July, pp. 1–19, 2018, doi: 10.3389/fpls.2018.00920.

[28] K. Bensch *et al.*, “Cladosporium species in indoor environments,” *Stud. Mycol.*, vol. 89, pp. 177–301, 2018, doi: 10.1016/j.simyco.2018.03.002.

[29] V. Sadrmanesh and Y. Chen, “Bast fibres: structure, processing, properties, and applications,” *Int. Mater. Rev.*, vol. 64, no. 7, pp. 381–406, 2019, doi: 10.1080/09506608.2018.1501171.

[30] S. Lakhundi, R. Siddiqui, and N. A. Khan, “Cellulose degradation: A therapeutic strategy in the improved treatment of Acanthamoeba infections,” *Parasites and Vectors*, vol. 8, no. 1, pp. 1–16, 2015, doi: 10.1186/s13071-015-0642-7.

[31] J. Summerscales, “A review of bast fibres and their composites: Part 4 ~ organisms and enzyme processes,” *Compos. Part A Appl. Sci. Manuf.*, vol. 140, no. October 2020, p. 106149, 2021, doi: 10.1016/j.compositesa.2020.106149.

[32] Z. Maundrill, “The Effects of Different Environmental Conditions on Hessian in Historic Fibrous Plaster Wads,” University of Bath, 2021.

[33] Industrial Plasters, “Jute Scrim,” *Industrial Plasters*, 2022. https://industrialplasters.com/collections/scrim-laths/products/jute-scrim (accessed Sep. 05, 2022).

[34] BSI Standards Publication, “BS EN 12390-5-2019 - TC--[2023-01-12--07-59-50 PM].pdf.” British Standards Institution, London, UK, 2019.

[35] P. E. Petersson, “Fracture energy of concrete: Method of determination,” *Cem. Concr. Res.*, vol. 10, no. 1, pp. 78–89, 1980.

[36] P. E. Petersson, “Crack growth and development of fracture zones in plain concrete and similar materials,” Lund, 1981. [Online]. Available: ISSN 0349-4985.

[37] S. Khalilpour, E. BaniAsad, and M. Dehestani, “A review on concrete fracture energy and effective parameters,” *Cem. Concr. Res.*, vol. 120, no. March, pp. 294–321, 2019, doi: 10.1016/j.cemconres.2019.03.013.

[38] A. Belaadi, S. Amroune, and M. Bourchak, “Effect of eco-friendly chemical sodium bicarbonate treatment on the mechanical properties of flax fibres: Weibull statistics,” *Int. J. Adv. Manuf. Technol.*, vol. 106, no. 5–6, pp. 1753–1774, 2020, doi: 10.1007/s00170-019-04628-8.

[39] M. Bekker, H. P. Huinink, O. C. G. Adan, R. A. Samson, T. Wyatt, and J. Dijksterhuis, “Production of an extracellular matrix as an isotropic growth phase of Penicillium rubens on gypsum,” *Appl. Environ. Microbiol.*, vol. 78, no. 19, pp. 6930–6937, 2012, doi: 10.1128/AEM.01506-12.

[40] K. A. van Laarhoven, H. P. Huinink, and O. C. G. Adan, “A microscopy study of hyphal growth of Penicillium rubens on gypsum under dynamic humidity conditions,” *Microb. Biotechnol.*, vol. 9, no. 3, pp. 408–418, 2016, doi: 10.1111/1751-7915.12357.

[41] A. V. Gusakov and A. P. Sinitsyn, “Cellulases from Penicillium species for producing fuels from biomass,” *Biofuels*, vol. 3, no. 4, pp. 463–477, 2012, doi: 10.4155/bfs.12.41.

[42] Y. B. Huang and Y. Fu, “Hydrolysis of cellulose to glucose by solid acid catalysts,” *Green Chem.*, vol. 15, no. 5, pp. 1095–1111, 2013, doi: 10.1039/c3gc40136g.

[43] S. H. D. Hulleman, J. M. Van Hazendonk, and J. E. G. Van Dam, “Determination of crystallinity in native cellulose from higher plants with diffuse reflectance Fourier transform infrared spectroscopy,” *Carbohydr. Res.*, vol. 261, no. 1, pp. 163–172, 1994, doi: 10.1016/0008-6215(94)80015-4.

[44] F. J. J. Segers, K. A. van Laarhoven, H. A. B. Wösten, and J. Dijksterhuis, “Growth of indoor fungi on gypsum,” *J. Appl. Microbiol.*, vol. 123, no. 2, pp. 429–435, 2017, doi: 10.1111/jam.13487.

[45] S. Mishra and N. Misra, “Efficacy of some triazoles and pyrimidine-2-one compounds against Chaetomium, Cunninghamella and Memnoniella found in deteriorating jute fibres,” *ScienceAsia*, vol. 35, no. 2, pp. 211–214, 2009, doi: 10.2306/scienceasial513-1874.2009.35.211.

[46] A. Nielsen and M. Morelli, “Measured temperature and moisture conditions in the roof attic of a one-and-a-half story house,” *Energy Procedia*, vol. 132, pp. 789–794, 2017, doi: 10.1016/j.egypro.2017.10.028.

[47] M. F. Sailer, E. J. van Nieuwenhuijzen, and W. Knol, “Forming of a functional biofilm on wood surfaces,” *Ecol. Eng.*, vol. 36, no. 2, pp. 163–167, 2010, doi: 10.1016/j.ecoleng.2009.02.004.

[48] D. Liu, B. Šavija, G. E. Smith, P. E. J. Flewitt, T. Lowe, and E. Schlangen, “Towards understanding the influence of porosity on mechanical and fracture behaviour of quasi-brittle materials: experiments and modelling,” *Int. J. Fract.*, vol. 205, no. 1, pp. 57–72, 2017, doi: 10.1007/s10704-017-0181-7.

[49] P. Reynaud, M. Saâdaoui, S. Meille, and G. Fantozzi, “Water effect on internal friction of set plaster,” *Mater. Sci. Eng. A*, vol. 442, no. 1-2 SPEC. ISS., pp. 500–503, 2006, doi: 10.1016/j.msea.2006.01.152.

[50] F. Y. Fan, “Evaluating the wetting and drying response of gypsum drywall subject to liquid water,” *Thesis, Univ. Toronto*, p. 60, 2017.

[51] R. Ireland, “Fibrous Plaster Ceiling Investigation: The Apollo Theatre Shaftesbury Avenue, London, Auditorium Ceiling.” Plaster & Paint, 2014.

[52] R. Clifford, “Maintaining Large Fibrous Plaster Ceilings,” *Buildingconservation.com*, 2019. https://www.buildingconservation.com/articles/fibrous-plaster-ceilings/fibrous-plaster-ceilings.htm (accessed Jan. 16, 2023).